DOE/ID/12079-7
ESL-37

Master

THE GEOLOGY OF THE BEOWAWE GEOTHERMAL SYSTEM, EUREKA AND LANDER COUNTIES, NEVADA

by

Eric M. Struhsacker

July 1980

EARTH SCIENCE LABORATORY DIVISION
UNIVERSITY OF UTAH RESEARCH INSTITUTE
420 Chipeta Way, Suite 120
Salt Lake City, Utah 84108

Prepared for the
DEPARTMENT OF ENERGY
DIVISION OF GEOTHERMAL ENERGY
Under Contract No. DOE/ID/12079

DISCLAIMER

NOTICE

This report was prepared to document work sponsored by the United States Government. Neither the United States nor its agent, the United States Department of Energy, nor any Federal employees, nor any of their contractors, subcontractors or their employees, makes any warranty, express or implied, or assumes any legal liability or responsibility for the accuracy, completeness, or usefulness of any information, apparatus, product or process disclosed, or represents that its use would not infringe privately owned rights.

NOTICE

Reference to a company or product name does not imply approval or recommendation of the product by the University of Utah Research Institute or the U.S. Department of Energy to the exclusion of others that may be suitable.

TABLE OF CONTENTS

LIST OF FIGURES, PLATES, AND TABLES

ABSTRACT

This report describes a geologic study undertaken to evaluate the nature of structural and stratigraphic controls within the Beowawe geothermal system, Eureka and Lander Counties, Nevada. The study is part of a comprehensive ongoing case study of the Beowawe geothermal system sponsored by the Division of Geothermal Energy of the Department of Energy under the Industry Coupled Program. This study includes geologic mapping at a scale of 1:24,000 and lithologic logs of deep Chevron wells.

Two major normal fault systems control the configuration of the Beowawe geothermal system. Active hot springs and sinter deposits lie along the Malpais Fault zone at the base of the Malpais Rim. The Malpais Rim is one of several east-northeast-striking, fault-bounded cuestas in north central Nevada. A steeply inclined scarp slope faces northwest towards Whirlwind Valley. The general inclination of the volcanic rocks on the Malpais dip slope is 5^{o} to 10^{o} southeast.

The Malpais scarp slope exposes normal faults on a northwest trend that predate the development of the Malpais scarp. An Oligocene to Miocene graben, presently confining the known geothermal system, developed along this trend. The north-northwest-trending Dunphy Pass Fault zone east of the sinter terrace is the eastern boundary of the graben. The western boundary of the graben appears to cross the Malpais Rim in Horse Heaven but is poorly exposed. A 1200 m-thick section of Miocene basaltic andesite, dacite, and basalt flows accumulated within the developing graben and covered a middle Tertiary

sequence of tuffaceous sediments, tuffs, and andesite flows, and the subjacent Ordovician Valmy Formation.

The Malpais Fault zone developed after the eruption of the Miocene volcanics; the normal faults controlling the scarp primarily strike east-northeast to east-west. However, these faults define two flexures in the overall east-northeast-trend of the Malpais Rim; The Geysers occur at one of these flexures. A set of steeply-dipping east-northeast and east-west-trending faults controlling the Malpais Rim scarp slope apparently carry hot fluid to the surface. Northwest and west-northwest-trending vertical faults may limit the northeastern and southwestern extent of modern surficial thermal activity. The intersections of these faults and the Malpais fault may serve as deep conduits for the geothermal system. At the southwest end of the terrace, the Malpais scarp curves to the southwest, whereas elements of the east-northeast fault set appear to continue westward into the valley, creating a subtle horst-like structure and permitting the westward migration of thermal fluids.

The deep Ginn and Rossi wells penetrate the Tertiary volcanics and the Valmy Formation. Hydrothermal alteration minerals in these wells are vertically zoned from a clay-calcite-quartz-pyrite assemblage above 600 m (2000 ft) of depth to a quartz-calcite-mixed chlorite and clay-pyrite-sericite-epidote assemblage below 1400 m (4500 ft). Alteration intensity is variable due to varying fracture and lithologic permeabilities and diverse lithologic compositions.

The faults controlling the Malpais scarp also served as conduits for hydrothermal fluids earlier in the evolution of the scarp. Uplift along the

Malpais scarp within and east of the Dunphy Pass fault zone exposes the Valmy Formation and a swarm of chalcedony-carbonate veins. Broad areas of silicification, argillization, and brecciation invade the Valmy formation and the Miocene volcanics. The intersection of these two major fault zones is, perhaps, a deep conduit for modern thermal fluids. A zone of anomalously low resistivity extends from the surface at the modern sinter terrace to 900 m (3000 ft) of depth within the Dunphy Pass Fault zone. The silicified zone presently appears to divert fluid laterally to the modern hot springs. Permeable zones of fractured Valmy Formation and volcanic rocks probably serve as satellite reservoirs at shallow to intermediate depths.

Regional heat flow data indicate that circulation of fluid to a deep reservoir is necessary to explain the high measured temperatures of 214°C encountered at a depth of 2880 m (9460 ft) in the Ginn well. Geologic evidence is inadequate to determine if the deep reservoir resides in the siliceous rocks of the Roberts Mountains thrust or within deeper carbonates.

INTRODUCTION

The Beowawe geothermal system, also known as The Geysers, lies 30 km (18.6 mi) southeast of Battle Mountain, astride the Lander-Eureka county line in the Whirlwind Valley of north-central Nevada (Figure 1). Beowawe ranks among the hottest of the numerous known geothermal systems in the Great Basin (Garside and Schilling, 1979). Several small geysers, hot springs, and fumaroles captured the attention of early settlers in the area. The geothermal system has built a large opaline sinter terrace along the fault-controlled Malpais Rim on the southeast margin of the Whirlwind Valley. The sinter terrace is about 75 m high and 850 m long by 30 m wide at the crest (Oesterling, 1962). The effluent of the system flows northeasterly down the Whirlwind Valley to the Humboldt River.

The vigorous geothermal activity prompted considerable exploration effort in Beowawe in the late 1950s for a resource amenable to electrical power generation. Magma Power Co., Vulcan Thermal Power Co., and Sierra Pacific Power Co., drilled a total of 12 shallow wells between 1959 and 1965 (Garside, 1974). Several of these wells tapped fluid in excess of 200°C at depths of less than 300 m (1000 ft) directly below the terrace. Two wells drilled for the Sierra Pacific Power Co. tested potential in fractures on the crest of the Malpais Rim. These wells all appear to have been designed to test the reservoir potential of the Malpais fault zone beneath the sinter terrace. This work, however, did not result in commercial energy production, and, in 1973, exploration activity resumed with the drilling of the Ginn No. 1-13 well by Chevron-American Thermal Resources, Inc. The 2915 m (9563 ft) Ginn well

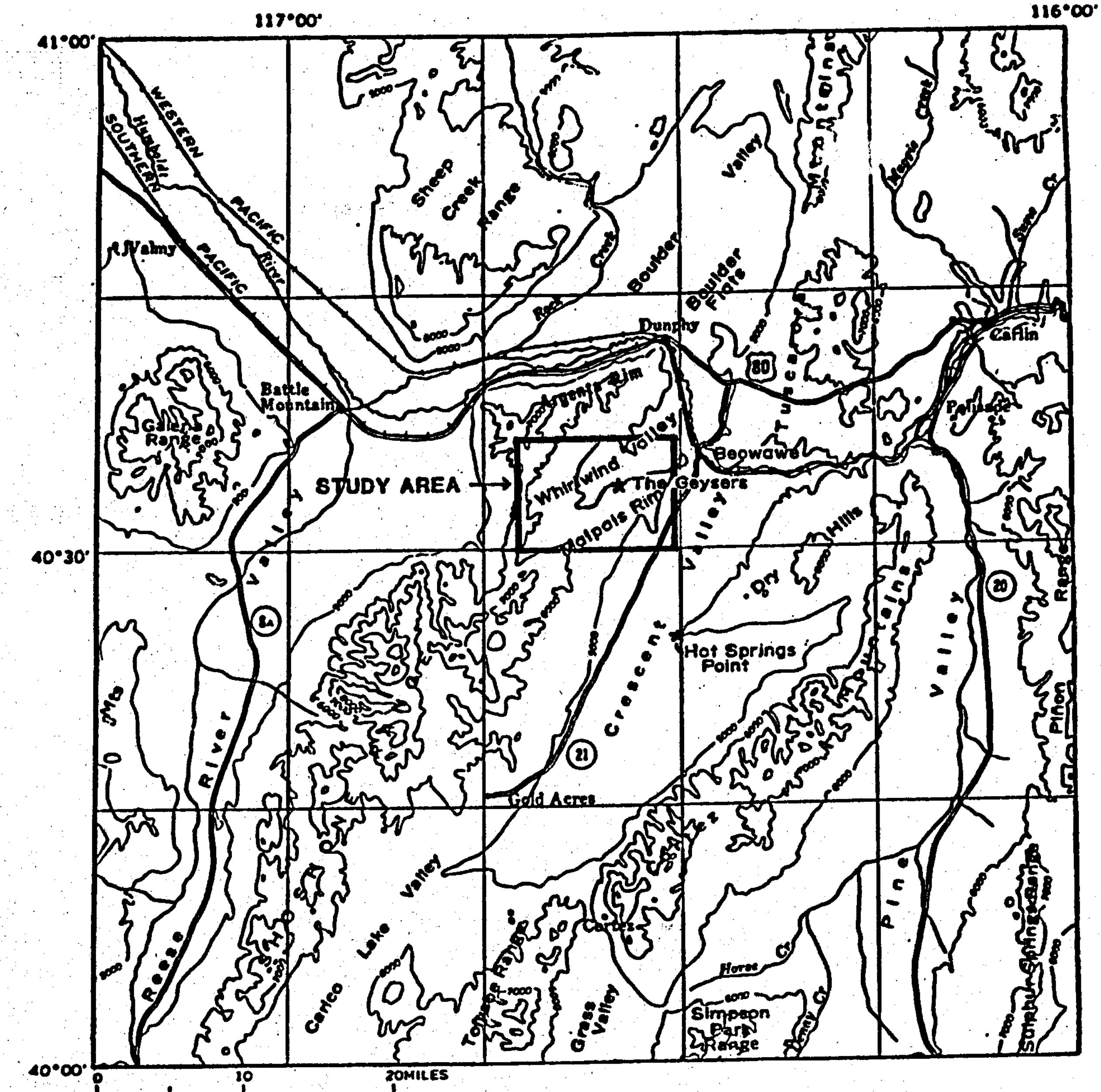

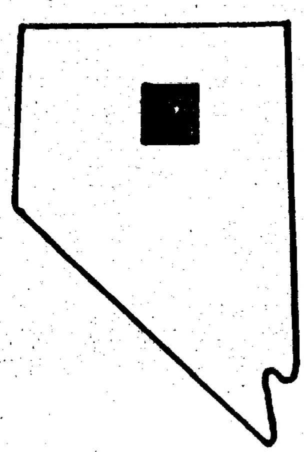

FIGURE 1 LOCATION MAP OF THE BEOWAWE GEOTHERMAL STUDY AREA. (BASE MAP MODIFIED FROM ZOBACK, 1979)

and the subsequent 1733 m (5686 ft) Rossi No. 21-19 well of Chevron U.S.A., Inc. tested an area 2.4 km (1.5 mi) west of the sinter terrace. Magma Energy, Inc. drilled the 1829 m (6000 ft) Batz No. 1 well at the base of the sinter terrace in 1975 (Zoback, 1979). The Chevron wells expanded the prospect area and presented the possibility of a deep target within the Malpais fault zone or subsidiary fractures.

Chevron Resources Co. and Getty Oil Co. are currently investigating the energy potential of the area. Each company has submitted geophysical, geological, and geochemical data to the U.S. Department of Energy as provided by contracts for geothermal reservoir assessment in the Industry Coupled Program. Ongoing studies by these groups and the Earth Science Laboratory of the University of Utah Research Institute point to the need for additional detailed structural and stratigraphic work in the vicinity of the geothermal system. This report describes the results of mapping at a scale of 1:24000 (Figure 2), includes summary lithologic logs of cuttings from the Chevron wells Ginn No. 1-13 and Rossi No. 21-19, and describes the nature and intensity of hydrothermal alteration at the surface and at depth. Interpretations of Chevron resistivity and shallow seismic data by Smith and others (1979) and Smith (1979), and major element analyses and K-Ar dates of volcanic rocks performed by Drs. S. H. Evans and F. H. Brown of the Department of Geology and Geophysics of the University of Utah and reported herein, contribute to the structural and stratigraphic models.

Previous Work

The first published account of geothermal activity at Beowawe appeared in

an article written by A. S. Evans for an 1869 issue of the Overland Monthly. T. B. Nolan and G. H. Anderson (1934) provided the first geologic description of the geothermal system and included analyses of three water samples. Oesterling (1960) subsequently prepared an unpublished geological appraisal of the Beowawe prospect for the Southern Pacific Company. He incorporated this report in a public presentation entitled "Geothermal Power Potential of Northern Nevada" (1962). His reconnaissance map includes the immediate prospect area at 1:2400 scale with cross sections and an account of the early drilling and well testing. Rinehart (1968) attempted to establish seismic signatures and short-time temperature histories of the water in three of the geysers. He also related the effects of the early exploration work on the Beowawe thermal features. More recently, Zoback (1979) integrated the generalized geology of the Malpais Rim and adjacent areas with the results of bipole-dipole resistivity, self potential, seismic noise, gravity, and magnetic investigations.

Additional summaries of the local geology, geochemistry, and exploration history appear in Garside (1974), Hose and Taylor (1974), Wollenberg and others (1975 and 1977), and Garside and Schilling (1979). Regional studies describing the Beowawe area include those of Stewart and Carlson (1976), Stewart and others (1977), and Roberts and others (1967). Reports by Gilluly and Gates (1965), Gilluly and Masursky (1965), Zoback (1978), and Zoback and Thompson (1978) provide valuable information from areas peripheral to the geothermal system. Olmstead and others (1973) list sources of geologic and hydrologic data for the Crescent Valley - Whirlwind Valley area.

GEOLOGIC SETTING

The Beowawe geothermal system lies near the axis of the Basin and Range physiographic province (Stewart and others, 1977). The Malpais Rim is one of several east-northeast-striking cuestas in north-central Nevada (Figure 1), and, with the Argenta Rim, forms the northern termination of the 320 km-long Shoshone Range. The Humboldt River truncates the northeast ends of the Malpais and Argenta Rims. North-northeast-trending normal faults dominate the regional structural terrain of north-central Nevada, giving rise to the major ranges and valleys (Figure 1). However, within the mapped area, the regional fault trend turns easterly to produce the observed cuestas. Major north-northwest-trending cross-fractures, occurring within the study area, laterally confine a sequence of middle Miocene calc-alkaline to alkaline flows. These flows comprise most of the outcrops in the mapped area and represent the central portion of an elongate middle Miocene volcanic field that overlies the Oregon-Nevada lineament and extends from southeast Oregon to central Nevada (Stewart and others, 1975; Zoback, 1978; and Zoback, 1979). The flows accumulated in north-northwest-trending grabens produced by middle Miocene rifting along the Oregon-Nevada lineament. Zoback (1978) named this structure the Northern Nevada Rift. In the Cortez and Roberts Mountains to the southeast of Beowawe, the rift structures confine swarms of parallel north-northwest-trending diabase dikes. Gilluly and Masursky (1965) believe that these dikes were the sources of the flows in those areas.

The volcanics of the Beowawe geothermal area lie unconformably on allochthonous lower Paleozoic siliceous eugeosynclinal rocks (Figure 2). In the

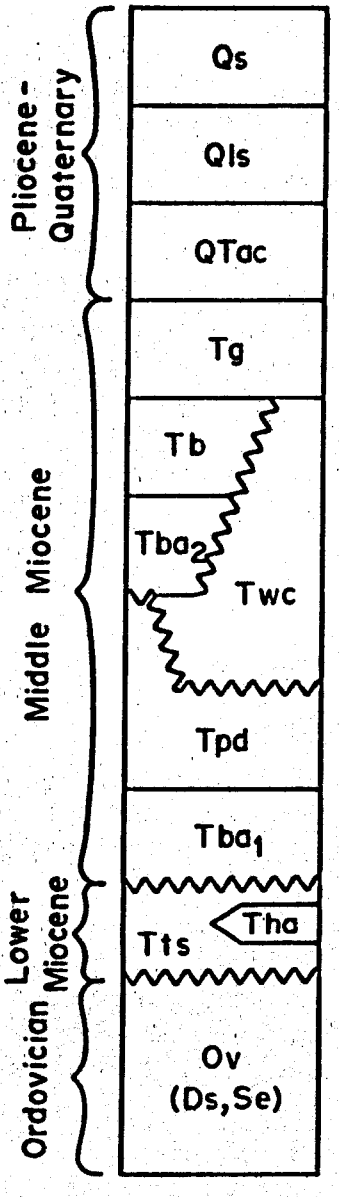

Qs – opaline sinter

Qls – landslide, probably Pleistocene

QTac – alluvium and colluvium

Tg – coarse gravel with Tb and Tba_2 cobbles

Tb – diktytaxitic, subophitic basalt flows

Tba_2 – subophitic basaltic andesite flows

Twc – White Canyon tuffaceous sediments (no Ov clasts)

Tpd – pyroxene dacite including porphyritic, aphanitic, and vitrophyric flows

Tba_1 – subophitic basaltic andesite and basalt flows

Tts – tuffaceous sediment with Ov clasts

Tha – hornblende andesite flows

Ov – Valmy Formation siliceous siltstone, chert, quartzite, quartz sandstone, and greenstone with possible tectonic slices of Slaven Chert (Ds) and Elder Sandstone (Se).

FIGURE 2 STRATIGRAPHIC COLUMN OF EXPOSED UNITS IN THE BEOWAWE AREA

vicinity of the study area, the siliceous rocks lie in fault contact upon the subjacent autochthonous carbonates along the Upper Devonian to Lower Mississippian Roberts Mountain thrust of the Antler Orogeny (Stewart and others, 1977). The main thrust and the many subsidiary faults as exposed in the Crescent Valley quadrangle have severely fractured and folded the upper plate while gently folding the lower plate (Gilluly and Gates, 1965). Thrust faults, folds, and younger sedimentary rocks related to several subsequent orogenies further complicate this complex structural terrain in peripheral areas.

Exposures of Paleozoic rocks within the mapped area are limited to the scarp slope of the Malpais Rim east northeast of The Geysers (Plate 1). Roberts and others (1967) and Zoback (1979) considered the siltstone, quartzite, chert, and siliceous conglomerate to be part of the Ordovician Valmy Formation. The Valmy, or its distal correlative, the Vinini Formation, appears in a similar structural setting on the north and east sides of the Argenta Rim outside the mapped area (Roberts and others, 1967). Extensive exposures of the Vinini occur in the Tuscarora Mountains immediately to the northeast of the Argenta and Malpais Rims. Thrust faults of the Antler Orogeny place the Valmy against the Devonian Slaven chert on the west side of the Argenta Rim (Stewart, 1969). The Valmy and the Slaven formations outcrop over large portions of the Mount Lewis area in the northern Shoshone Range, to the southwest of Whirlwind Valley (Gilluly and Gates, 1965). These rocks, along with lesser amounts of the feldspathic Silurian Elder Sandstone on Mount Lewis, comprise the Roberts Mountain allochthon in the Beowawe vicinity. The Ginn No. 1-13 and Rossi No. 21-19 wells located at the base of the Malpais Rim penetrate rocks interpreted as Valmy Formation below depths of 1350 m (4500

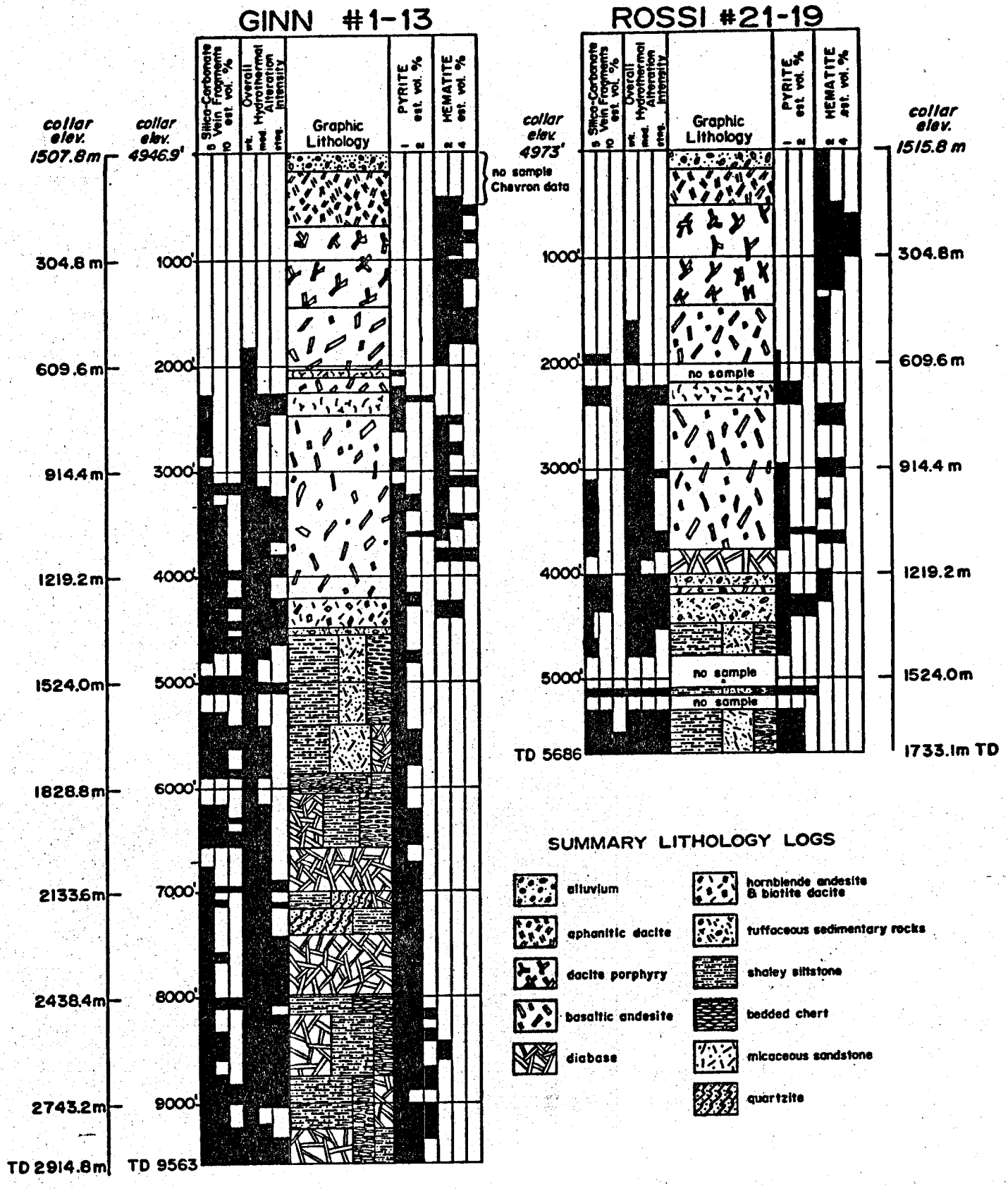

FIGURE 3 SUMMARY LITHOLOGIC LOGS OF THE GINN 1-13 AND THE ROSSI 21-19 WELLS.

TABLE 1

K-Ar Age Dates for Tertiary Volcanics
(sample locations on Plate I)

Sample No.	Unit	Material Dated	Weight (gms)	%K	Moles/gm Ar^{40} ($\times 10^{11}$) Rad	$\%Ar^{40}$ atm	Age (m.y.)
NV/BW 79-85	biotite dacite	Biotite	0.34495	6.71	45.610	24	38.8 ± 1.3
NV/BW 79-84	hornblende andesite	Biotite	0.40630	6.64	44.934	18	38.6 ± 1.3
NV/BW 79-180	pyroxene dacite	Plagioclase	2.08253	0.89	2.499	51	16.1 ± 0.6
NV/BW 79-154	pyroxene dacite	Sanidine	0.52108	6.54	18.2989	32	16.1 ± 0.5
NV/BW 79-104	young basaltic andesite	Whole Rock	3.32479	1.27	3.659	53	16.6 ± 0.7
NV/BW 79-104	young basaltic andesite	Whole Rock	3.01703	1.27	3.692	61	16.7 ± 0.7
NV/BW 79-21	late basalt	Whole Rock	5.06662	0.76	2.172	69	16.3 ± 0.8
NV/BW 79-112	late basalt	Whole Rock	2.13457	0.83	2.390	68	16.5 ± 0.8

Constants Used:

$\lambda\beta = 4.962 \times 10^{-10}$/yr.

$\lambda_\epsilon = 0.581 \times 10^{-10}$/yr.

$K^{40}/K_{Tot.} = 1.167 \times 10^{-4}$ Mole/Mole

Analyst: S. H. Evans

ft) (Plate 1 and Figure 3). However, horizons of a dirty sandstone suggest that tectonic slices of Elder Sandstone may lie within the section. Quantities of black and shaly siltstone resemble the Vinini Formation. Small windows in the allochthon peripheral to Beowawe expose carbonates of the eastern miogeosynclinal assemblage. The carbonates occur neither at the surface in the mapped area nor at the depths penetrated by the drill holes. However, one may presume that they occur at greater depths throughout the area.

Several large Mesozoic felsic stocks intrude Paleozoic and Mesozoic sedimentary rocks in the Cortez Mountains, whereas numerous small Lower to middle Tertiary felsic stocks intrude lower Paleozoic rocks in the Shoshone Range south of the study area (Muffler, 1964; Gilluly and Masursky, 1965; Gilluly and Gates, 1965).

STRATIGRAPHY

Ordovician Valmy Formation

The Valmy Formation, exposed along the Malpais scarp, consists predominantly of light grey siliceous siltstone with significant amounts of quartzite, sandstone, bedded chert, and siliceous conglomerate. Zoback, (1979) Roberts and others, (1967) Gilluly and Gates (1965) provide a detailed petrographic discription of the Valmy Formation in the Mount Lewis area. Petrographically, the siltstone contains quartz grains of uniform size with minor detrital feldspar and mica. It exhibits a mosaic texture with lobate, sutured grain boundaries and pervasive overgrowths of quartz. The siltstone grades into a medium- to coarse-grained white quartzite. Good exposures of

these rocks occur in sections 10, 15, and 16, T31N, R48E, where the quartzite forms prominent east-northeast-trending outcrops, and near the Red Devil mine in section 6, T31N, R49E. Shearing related to Paleozoic tectonism and Tertiary tensional fracturing generally obscures the true attitude of the bedding units. Tectonism has also obscured the stratigraphic relationships and thickness of the unit though Roberts and others (1964) determined that the Valmy is at least 2400 m thick in Eureka County. Gilluly and Gates (1965) suggest that the unit may approach 7500 m in thickness in the Mount Lewis area.

Chert layers of variable thicknesses occur sporadically within the siltstone. Open-pit barite mine development and extensive dozer cuts in sections 11 and 12, T31N, R48E reveal bedded chert horizons in excess of 30 m thick dipping approximately 20 degrees to the east-southeast. The chert is light grey, black, brown, or light green with individual beds 5 to 15 cm thick. The green chert commonly occurs as thin interbed films up to 1 cm thick, although some exposures contain alternating layers of green and black or brown chert several centimeters thick. Bedded chert exposures in the southern half of the northeast quarter of section 11 are predominantly green. The cherts also contain sporadic green and black shaley partings, as well as highly variable thicknesses of bedded nodular barite. The nodules are commonly less than 1 cm in diameter and occur in a light green shaley or cherty matrix.

Occasional exposures of clean quartz sandstone occur in close association with a silicious conglomerate. The sandstone is very clean with subround to

round, fine to medium grains. Zoback (1979) distinguished a chert conglomerate with poorly sorted subangular to subround variegated clasts from a pebble conglomerate with well sorted, rounded siliceous pebbles of a white, grey, or black color. These rocks are well exposed in the Red Devil Mine workings, but appear only as float to the southwest along the Malpais scarp front.

Tectonism has severely fractured the Valmy rocks and produced some cataclastic texture and foliation. Quartz and chalcedony overgrowths have also modified the original textures. The abundant red coloration of the Valmy noted by Zoback (1979) along the Malpais scarp slope is most likely hematite and limonite related to late Tertiary and Quaternary hydrothermal activity. The limonitized zone extends southwest to The Geysers area (Figure 9).

Old Tuffaceous Sedimentary Rocks

A regionally widespread section of felsic tuffaceous sedimentary rocks rests unconformably on the Valmy Formation (Plates 1 and 2). Evidence for the unit exists in the float wherever the Valmy crops out on the Malpais Rim, although exposures are poor due to the incompetent nature of the interbedded sedimentary rocks and tuffs. The tuffaceous unit typically forms a gentle slope compared with the steeper exposures of the Valmy Formation and the overlying lava flows. Fresh exposures of the unit occur in the gravel pits to the south of the Red Devil Mine and on an oversteepened slope immediately to the east of the toe of the prominent Quaternary landslide on the Malpais scarp slope (Zoback, 1979). Two additional small exposures occur on the scarp slope immediately to the east and west of the barite mine in section 12. Maximum

observed thicknesses range from 125 m in the Rossi well to 70 m on the Malpais scarp slope.

The tuffaceous sedimentary rocks outcrop widely on the eastern, northern, and western scarp slopes of the Argenta Rim (Stewart and others, 1977). Gilluly and Gates (1965) and Gilluly and Masursky (1965) observed similar gravelly tuffaceous rocks lying between Paleozoic rocks and the middle Miocene basaltic andesite pile in the Mount Lewis area and on the Cortez Mountains. Tuffaceous sedimentary rocks form subdued hills to the east of Beowawe along the Humboldt River (Stewart and Carlson, 1976). These deposits are probable continuations of the Red Devil exposure.

The Ginn well penetrates the tuffaceous sedimentary unit at depths from 1257 to 1275 m (4190 to 4250 ft) and from 1320 to 1365 m (4400 to 4550 ft) of depth (Figure 3); a hornblende-biotite-andesite flow occupies the intervening interval. The Rossi well cuts a similar section with tuffaceous sediment from 1200 to 1248 m (4000 to 4160 ft) and 1272 to 1335 m (4240 to 4450 ft). The intervening lava flow crops out only along the glide plane on the west side of the Quaternary landslide in the north-central part of section 15 (Plate 1). Cobbles of the flow rock are common in many exposures of the tuffaceous sedimentary section in the area. A potassium-argon dating of biotite phenocrysts suggests an age of 38.7 ± 1.3 m.y. (Table 1, sample NV/BW79-84). Cobbles of a closely associated biotite dacite yield an age of 38.8 ± 1.3 m.y. from separated biotite phenocrysts (Table 1, Plate 1).

The tuffaceous sedimentary rock unit is composed of gravel, sand, and silt in a tuffaceous matrix interbedded with thin airfall or water-lain tuff

layers. Cross bedding in the gravels suggests fluvial deposition. The gravels are most conspicuous in subdued outcrop leaving an abundance of rounded to subangular siliceous pebbles in a bentonitic soil. The pebbles are predominantly chert, quartzite, siliceous siltstone, and sandstone. The black, brown, grey, and green cherts of the Valmy formation are distinctive. Sporadic concentrations of cobbles and boulders from the Valmy quartzite and siliceous conglomerate appear in the float, and a variety of middle Tertiary felsic and mafic volcanic clasts are also common. These clasts are clearly distinguishable from the local middle to late Miocene volcanics. The tuffaceous matrix contains fine- to medium-grained feldspathic sand, broken feldspar, quartz, and mafic crystals, and variable amounts of fresh to partly altered glass shards. Carbonate is common as a cement. The ash layers are buff to grey and range up to a meter in thickness, containing well preserved brown glass shards with minor admixed fine-grained detrital material.

The interbedded hornblende biotite andesite contains about twenty percent plagioclase, fifteen percent hornblende, and three percent biotite as anhedral phenocrysts in a light grey microlitic to aphanitic groundmass. The plagioclase phenocrysts are commonly 2 to 4 mm in length and occasionally attain 10 mm in length. The larger plagioclase phenocrysts display well developed zoning. The hornblende phenocrysts vary from 1 to 10 mm in length. Biotite forms scattered books about 5 mm in diameter. Magnetite, a common accessory mineral, occurs as finely disseminated subhedral grains. Magnetite and biotite commonly replace the hornblende phenocrysts as probable deuteric alteration products. The groundmass is thoroughly argillized in the drill

hole intercepts and in much of the outcrop. However, portions of the outcrop contain well preserved groundmass and plagioclase phenocrysts.

Middle Miocene Volcanic Rocks

A thick sequence of volcanic flows covers the tuffaceous sediments in the vicinity of The Geysers (Plates 1 and 2). The cuesta scarp slopes expose up to 600 m of the volcanic section in Horse Heaven to the southwest of The Geysers and on the northern side of the Argenta Rim. The flows form cliffs on the scarp slopes and dip gently to the southeast at five to ten degrees. The Ginn and Rossi wells penetrate 1200 m of volcanics above the tuffaceous sediments. The locally great thickness of the section contrasts with normal regional thicknesses of less than 300 m (Zoback, 1979).

Our mapping, petrography, and petrochemistry indicate considerable compositional variability through the Malpais Rim section and, in conjunction with the deep drilling record, allow the subdivision of the lava flow sequences previously mapped only as basaltic andesite (Figure 2). The volcanic section includes: 600 m of basaltic andesite with minor basalt, 300 m of pyroxene dacite, 40 m of tuffs and tuffaceous sedimentary rocks, 100 m of basaltic andesite, and 10 to 30 m of basalt in ascending order above the lower to middle Miocene tuffaceous sedimentary rocks. Basaltic andesite predominates throughout the volcanic field south of the Humboldt River (Gilluly and Masursky, 1975; Gilluly and Gates, 1975), although several rhyolite flows occur in the Cortez Mountains. Rhyolite flows and domes with basalt cap flows increase in abundance relative to the basaltic andesites between the Humboldt River and the Oregon - Nevada border (Stewart and

Carlson, 1976). Major element compositions as plotted in Figure 7 indicate that the volcanic sequence in the study area has calc-alkaline and alkaline components. The following sections will discuss the details of the major rock types of the volcanic section in the vicinity of the geothermal system.

Old Basaltic Andesite

The old basaltic andesite unit is a thick pile of lava flows with occasional interbedded thin horizons of felsic tuff and volcanic agglomerate. The only recognized outcrop of the unit exposes approximately of 300 m of flows on the scarp slope of the Malpais Rim in Horse Heaven (Plates 1 and 2). A small exposure of tuffaceous sedimentary rock (Stewart and others, 1977) marks the bottom of the basaltic andesite unit in this locality. The Ginn and Rossi wells, however, penetrate much thicker basaltic andesite sections of 828 m and 765 m respectively, substantiating Zoback's (1979) proposed northwest-trending middle Miocene graben between Horse Heaven and White Canyon (Figure 3).

The unit is, predominantly, a medium-grey pyroxene-bearing basaltic andesite with minor olivine. Plagioclase occurs as microlites and as 1 to 4 mm-long phenocrysts with intergranular clinopyroxene. The rock also contains finely disseminated accessory magnetite along with occasional apatite. Vesicular zones locally contain chalcedony, calcite, chlorite, clays, and zeolites.

The deep wells intercept tuffaceous sedimentary rocks at depths between 600 and 702 m. The tuffs contain angular quartz and feldspar fragments in a matrix of clay and carbonate. Several volcanic agglomerate horizons appear in

the Horse Heaven outcrop, but are difficult to recognize in drill cuttings. The coarse angular basaltic andesite clasts rest in a clay-rich matrix and are generally well weathered. However, the spread in SiO_2 values from samples of the basaltic andesite sequence taken from drill cuttings and one outcrop indicate a range in rock type from basalt to andesite[1].

The sample density is insufficient to identify any vertical trends in rock composition. Petrographic evidence indicates that the majority of the sequence sampled in the drill holes resembles the flows which, at a depth of 975 m (3200 ft), yielded an SiO_2 value of 54.5 percent of the total oxides (Table 2).

The drill cuttings (Chevron, 1979) reveal intermittant zones of moderate to intense hydrothermal alteration throughout the basaltic andesite sequence. The tuffaceous rocks are strongly altered as well. A later section of this report will describe the nature of this alteration.

Pyroxene Dacite

The scarp slopes of the Malpais and Argenta Rims expose prominent cliffs of pyroxene dacite lava flows. The flow sequence attains its maximum thickness of 300 m in the vicinity of The Geysers and the Chevron wells (Plate 2). The flows appear to have filled a north-northwest-trending graben now partly exposed in both the Malpais and Argenta scarps. The dacite section

[1]Subdivisions regardless of suite taken from Cameron and others, (1980): Basalt (53<% SiO_2), basaltic andesite (53-56% SiO_2), andesite (56-63% SiO_2),dacite (63-70% SiO_2), and rhyolite (>70% SiO_2).

TABLE 2

Major Element Contents of Miocene Volcanics
(samples representative of each unit)

	diabase	old basaltic andesite	pyroxene dacite porphyry	aphanitic dacite	young basaltic andesite	late basalt
	Ginn 1-13 6740	Ginn 1-13 2660	NV/BW 79.73	NV/BW 79.102	NV/BW 79.177	NV/BW 79.112
SiO_2	49.30	58.50	66.64	62.33	54.50	48.77
TiO_2	1.00	1.49	.78	.91	1.26	1.48
ZrO_2	.01	.02	.04	.04	.02	.01
Al_2O_3	15.19	13.31	13.37	13.94	16.19	16.29
Fe_2O_3	2.04	2.24	2.84	3.04	2.30	1.35
FeO	6.26	6.87	3.59	5.10	7.05	9.64
MnO	.17	.14	.04	.15	.16	.20
MgO	7.49	2.09	.91	.93	4.07	7.77
CaO	12.65	5.51	1.90	3.35	8.94	9.53
SrO	.03	.03	.02	.03	.03	.04
BaO	.03	.08	.16	.19	.07	.06
Na_2O	2.60	3.50	3.11	3.45	3.21	2.67
K_2O	.49	2.73	4.68	4.40	2.04	.96
P_2O_5	.20	.44	.17	.22	.39	.50
H_2O+	N.D.	N.D.	1.76	1.73	N.D.	.00
SO_3	N.D.	N.D.	N.D.	.02	N.D.	.04
TOTAL	97.46	96.95	100.01	99.83	100.13	99.11
Analyzed by:	ICP[1,4]	ICP[1,4]	XRF[2,4]	XRF[2,3]	ICP[1,4]	XRF[2,4]

[1]Analyst: R. Kroneman; ICP analysis determines total Fe only.

[2]Analysts: F. Brown and J. Mason

[3]FeO determined by the ammonium metavanadate back-titration method (S. Evans, analyst).

[4]FeO/Fe_2O_3 ratio inferred from FeO analyses of samples representative of each unit.

thins abruptly to a maximum thickness of 60 m across the eastern graben boundary fault at White Canyon. The unit maintains its maximum thickness as it extends southwestward to an abrupt termination along the western graben boundary fault. The graben boundary is exposed on the Malpais scarp slope in Horse Heaven and on the dissected Argenta dip slope in the northwest quarter of section 15, T31N, R47E. The graben margin in Horse Heaven juxtaposes the pyroxene dacite against the old basaltic andesite. Spurck (1960) and Willson (1960) mapped large areas of flows on the Argenta Rim and the northeast end of the Malpais Rim that are correlative with the pyroxene dacite unit. The petrographic and outcrop characteristics of the Shoshone Andesite of their reports are essentially identical to those of the pyroxene dacite described in this report. Potassium-argon dates of plagioclase phenocrysts from the middle of the dacite section indicate an age of 16.1 $\pm$ 0.6 m.y. (Table 1, Plate 1).

The pyroxene dacite unit displays considerable compositional and textural variability throughout the section. The cliffs of the Malpais and Argenta Rims are dominantly glomeroporphyritic pyroxene dacite, which we refer to as the dacite porphyry. The cliffs consist of at least four fifty m-thick flows that display a crude columnar, spheroidally weathered jointing. One possible source for these flows occurs at the western graben margin south of Horse Heaven, where a vertical dike follows the boundary fault to the surface. The flows are light brown to grey on fresh exposures and weather to a deep red brown. Phenocryst clots comprise ten to thirty percent of the rock. The clots typically contain several phenocrysts of plagioclase, clinopyroxene, olivine, magnetite, and apatite. The proportion of phenocrysts and their degree of agglomeration decreases irregularly upward through the pile of

flows. The corners of most plagioclase phenocrysts are rounded by resorption; pyroxene and olivine commonly appear to embay the plagioclase as well. Occasional flows display feldspar overgrowths on plagioclase phenocrysts. The plagioclase is usually fresh, whereas the pyroxene and, in particular, the olivine may be altered. Some secondary minerals, including chlorite, calcite, chalcedony, smectites, iddingsite, magnetite, and hematitic limonite, are most likely related to the deuteric alteration of the phenocrysts.

The groundmass of the pyroxene dacite is typically aphanitic-crystalline to glassy with variable amounts of microlites. Irregular networks of fine-grained quartz and feldspar commonly enclose glassy patches. Some horizons reveal incipient perlitic textures with secondary clays occupying concentric fractures. At least two distinct horizons contain abundant spheruloids of devitrified dacite in a matrix of fresh or weathered dacite. The spheruloids range from 1 to 10 cm in diameter and form a nodular grus upon the weathering of the flow unit. Phenocrysts commonly overlap the spheruloid boundaries and are fresh to weakly altered. Outcrops of spheruloidal flows occur throughout the Malpais and Argenta Rim areas, but the best exposures appear in the cut of the eastern geyser terrace access road and on the Malpais Rim crest in the eastern half of Section 3, T30N, R47E. A black vitrophyre with phenocrysts similar to those of the dacite porphyry marks the top of this sequence. The vitrophyre unit contains several spheruloidal horizons.

A glassy flow sequence, termed the aphanitic dacite, lies conformably on the dacite porphyry. Numerous red brown aphanitic flows interfinger with black aphanitic dacite flows that display a dense platey jointing controlled

by fluidal banding. The red brown flows contain variable amounts of microlites that produce a trachytic texture in the uppermost of these flows. Sparse phenocrysts resemble those of the dacite porphyry. The flows in this sequence are typically 3 to 5 m thick. Blocks from the red brown flows comprise much of a thin volcaniclastic horizon exposed on the east wall of White Canyon. This horizon may be either an interflow rubble zone, a volcanic agglomerate, or a paleo-colluvium on the east margin of the Miocene graben. Unusually erratic joint patterns and intense hematitization of these flows on the upper floor of White Canyon suggest possible vents for the aphanitic dacite flow sequence along the eastern graben margin.

Major element analyses support the use of the term dacite to characterize the flow sequences just described (Table 2). SiO_2 for the dacite porphyry ranges from 65 to 68 percent, whereas the flows of the aphanitic dacite sequence approach the composition of andesite with decreasing age.

White Canyon Tuffaceous Sedimentary Rocks

A thin unit of tuffaceous sedimentary rock and air fall tuff lies unconformably on the pyroxene dacite. The most extensive exposure of the unit occurs on the upper floor of White Canyon with approximately forty meters of well-bedded buff to light gray tuffaceous sandstone, siltstone, poorly consolidated ash, and porcellanite (Plate 1). Normal faulting along the eastern margin of the middle Miocene graben has downdropped and folded the tuffaceous unit into a gentle syncline. The unit thins to less than thirty meters as it extends southwestward beneath a cap of basalt. Cavities excavated by erosion and animals occasionally provide exposures of the

basalt-tuff contact, but basalt talus and colluvium generally obscure the incompetent tuffs. Tuff fragments near animal burrows and bentonitic soils are the principal clues to the location of the tuffaceous unit. Deep gullies have exposed the unit on the lower reaches of the Argenta dip slope beneath the basalt cap or similar basaltic andesite flows, but the tuffaceous sediment unit appears to pinch out to the northwest. A pink to gray nonwelded pumice-lithic tuff appears at the top of the unit on the south and east sides of the Argenta dip slope. Erosional and constructional topography, on the pyroxene dacite, and post-tuff erosion account for considerable variability in the areal distribution and thickness of the tuffaceous unit.

The bulk of the section is composed of buff-colored tuffaceous sandstone. The sandstone contains pyroxene dacite and old basaltic andesite clasts, broken quartz and feldspar phenocrysts, and abundant subaligned brown to black glass shards with a few intact bubble walls. Rare fragments of carbonized wood also appear in the sandstone. Thin interbedded grey pyroclastic and siltstone horizons, containing well-preserved shards with occasional phenocryst fragments, interfinger with the sandstone. Calcite is the dominant cement and thoroughly permeates certain horizons forming a coarse-grained mosaic pattern. Interbedded porcelanite layers up to ten cm thick along with the fine bedding suggest a lacustrine environment of deposition for the unit. The pumiceous-lithic tuff of the Argenta Rim contains more than sixty percent fresh pink to grey rhyolitic pumice clasts with ten percent black obsidian fragments in a shard-rich matrix. The large proportion of pumice clasts to finer matrix suggests substantial winnowing by fluvial or wave action. These

tuffaceous materials strongly resemble the older tuffaceous sediment unit but do not contain pre-Miocene clasts.

Young Basaltic Andesite

A sequence of five to eight basaltic andesite flows lies unconformably upon the White Canyon unit or the pyroxene dacite and caps the dip slopes of the Malpais and Argenta Rims (Plate 1). The flow sequence attains its maximum thickness of 300 m immediately south of Horse Heaven and tapers to the south for ten km along the east flank of the Shoshone Range (Gilluly and Gates, 1965). The basaltic andesite caps the Malpais Rim east of White Canyon with a thickness of 40 m. The unit is also widespread on the Argenta dip slope reaching thicknesses of 150 m. The flows range from 2 to 16 m in thickness and display crude columnar or blocky jointing. Deep gullies and canyons cut the cuesta dip slopes, but erosion of the original constructional flow surface has been minimal. Therefore, complete exposures of the basaltic andesite section are common.

Similar basaltic andesite flows are widely distributed in varying quantities throughout the northern Nevada rift. Gilluly and Masursky (1965) describe 105 m of basaltic andesite and basalt flows on the dip slope of the Cortez Mountains and suggest that diabase dikes exposed on the scarp slope served as conduits feeding the flows. Zoback (1978) describes a 400 m-thick basaltic andesite section beneath the rhyolites and basalts of the Midas trough area north of the Humboldt River. The character of those basaltic andesite occurrences strongly resembles that of the flows in the Beowawe area.

Post-volcanic faulting has apparently fragmented a major regional flow sequence.

A whole rock potassium-argon dating of basaltic andesite cap flow, preserved in slump blocks to the east of the Quaternary landslide, suggests an age of 16.7 $\pm$ 0.7 m.y. (Table 1). McKee and Silberman (1971) report a whole rock date of 16.3 m.y. from basaltic andesite on the east flank of the Shoshone Range south of Beowawe. Other reported basaltic andesite dates from the northern Nevada rift range from 14.5 to 16.3 m.y. (McKee and others, 1971).

The dark gray basaltic andesites contain fifty percent euhedral plagioclase laths with twenty percent intergranular anhedral pyroxene, twenty percent intersertal brown glass, five to ten percent magnetite, and minor olivine. Plagioclase and pyroxene grains are commonly less than one mm in length, but isolated phenocrysts up to five mm in length also occur. Some of the flows are highly vesicular with sporadic calcite, clay, chalcedony, and zeolite fillings. One of the flows within the section contains intergranular cavities forming a diktytaxitic texture.

The composition of the basaltic andesite resembles the average andesite of Nockolds (1954), but is lower in SiO_2 than the average of Chayes (1969). The SiO_2 contents of several samples from the Malpais and Argenta Rims range from 52 to 56 percent (Table 2).

Late Basalt

A thin sequence of one to three basalt flows caps portions of the Malpais and Argenta dip slopes (Plate 1). The basalt, between White Canyon and Horse Heaven, lies unconformably on the middle Miocene tuffaceous sediments. The flows occupy the drainages and basins on a subdued but irregular erosional surface developed on the tuffaceous sediment. Much of this exposure consists of one 2 m-thick flow displaying a crude columnar to blocky jointing. Frost action and slumping of the underlying tuffaceous sediments has reduced the thin flow unit in some areas to a pile of jumbled basalt blocks on a bentonitic soil. Subdued exposures of the basalt occur on the floor of the west end of Whirlwind Valley where two flows lie directly on the trachytic dacite and locally on intervening patches of tuff. The basalt flows, with two to three subjacent basaltic andesite flows, extend northward and northwestward from the lower slopes to the crest of the Argenta Rim. The basalt does not extend to the western and southwestern portions of the Argenta Rim due to recent erosion and local topographic highs during the eruption of the flows.

Two new whole rock K-Ar dates of the basalt exposed on the Whirlwind Valley floor and on the Malpais dip slope indicate an age of 16.3 to 16.5 $\pm$ 0.8 m.y., essentially the same age as the young basaltic andesite (Table 1). The valley flow and the flow capping the Malpais dip slope between White Canyon and Horse Heaven are essentially identical in composition (Table 2) and in thin section. The basalt cap flows, sampled at five localities on the Malpais and Argenta dip slopes, have SiO_2 contents ranging from 47.6 to 48.7 percent. These data refute Zoback's hypothesis (1979) that the valley flows

are correlative with a 10 m.y. old basalt flow capping the Sheep Creek Range dated by McKee and Silberman (1970).

The basalt is dark gray to black and weathers to dark brown. The rock displays a distinctive diktytaxitic texture that is easily recognized in hand sample. The minute inter-crystal cavities are commonly devoid of secondary minerals, however, thin vesicular horizons at the tops of the flows contain secondary calcite, silica, and clays. The typical subophitic textured basalt occasionally exhibits an ophitic texture. Euhedral plagioclase microlites and abundant phenocrysts, up to 5 mm in length, lie partly enclosed by subhedral phenocrysts of clinopyroxene and sporadic subhedral phenocrysts of olivine. Magnetite is a common accessory mineral as fine euhedral disseminations. The primary minerals are usually fresh with the exception of olivine, which is often altered to iddingsite.

Diabase Dikes

The Ginn well penetrates diabase over several intervals within the Valmy Formation below 1615 m (5300 ft) (Figure 3). Four samples of diabase cuttings, selected from unaltered to weakly altered intervals in the bottom 1280 m (4200 ft) of the hole, yield SiO_2 contents ranging from 47.2 to 50.8 percent. Basalts with SiO_2 contents in this range occur in the older basaltic andesite sequence and in the late basalt. Muffler (1964) sampled a diabase dike exposed on the scarp slope of the Cortez Mountains, which contained very similar amounts of major and immobile elements. The compositional similarity of the diabase cuttings from the Ginn well to the exposed dikes of the Cortez Mountains and the overlying flow sequences at Beowawe and the Cortez Mountains

suggests that a swarm of middle Miocene dikes lies beneath the Whirlwind Valley. In support of this possibility, Swift (1979) attributes a north-northwest-striking electrical anisotropy, observed in a Chevron MT survey at the Beowawe geothermal prospect, to bodies of conductive Valmy country rock confined between resistive diabase dikes.

Late Tertiary Gravels

Approximately 10 to 20 m of gravel lie on the dip slope of the Malpais Rim between White Canyon and Horse Heaven (Plate 1). The gravels lie unconformably on the White Canyon tuffaceous sedimentary rocks and late basalt and, to the south along the east flank of the Shoshone Range, overlies the dacite vitrophyre sequence and young basaltic andesite. The gravels do not occur on the Argenta dip slope. The uniform thickness of the unit suggests deposition on a surface of low relief. The unit includes debris from the young basaltic andesite and basalt units described above. The clasts range from sand to cobbles in size and are subrounded to well rounded.

The distribution, geometry, and composition of the gravel unit suggest that it predates the uplift of the Malpais cuesta (Zoback, 1979). The gravels appear to have filled a depression created by subsidence within the north-northwest-striking graben during and, perhaps, after Miocene volcanism. The structural details of this graben appear in a later section of this report.

Tertiary-Quaternary Landslides

A very striking lobate landslide of probable Pleistocene age extends 2 km from a detachment zone high on the Malpais scarp slope to the Whirlwind Valley

floor approximately 3 km east of The Geysers (Plate 1). The scarp face of the landslide exposes basaltic andesite and the uppermost pyroxene dacite, whereas the glide plane of the landslide lies in the Oligocene to early Miocene tuffaceous sediment.

To the east of the young slide, large mappable blocks of basaltic andesite, lying on the older tuffaceous unit, have slumped toward the valley in a step-like fashion. The stratigraphy is well preserved in these blocks. Other slump blocks of this type appear at the base of the Malpais scarp slope between the barite mine and the Red Devil Mine. Erosion has modified the shape of the slump blocks in this area.

Larger slump blocks have separated from the Malpais scarp slope in Horse Heaven. Here, a one- by two-kilometer block has detached from the scarp along a north-south fracture at the convex scarp flexure that marks the mouth of Horse Heaven. A 7 km-long segment of the Malpais scarp crest, in the southwestern part of Horse Heaven, has slumped toward the valley. The blocks in Horse Heaven have rotated toward the valley producing dips of 15 to 50 degrees on the Tertiary lava flows and, probably, covering the traces of the range front fault.

Quarternary Siliceous Sinter

Siliceous sinter produced by hot spring and geyser activity at The Geysers covers a mappable area of about two square kilometers along the base of the Malpais Rim (Plate 1). Thermal activity has built a sinter terrace approximately 60 m thick. Nolan and Anderson (1934) and Zoback (1979) provide detailed descriptions of the sinter deposit. The sinter is typically opaline

with minor clays, carbonates, and sulfates. The sinter terrace exhibits prominent layering of cemented sinter clasts and massive sinter. The unit contains significant quantities of pyroxene dacite colluvium slumped from the Malpais scarp slope. Clastic sinter horizons, incorporated colluvium, and cavities formed after organic material create porosity in the terrace.

The prominent terrace appears to be a product of the rapid deposition of sinter as evidenced by the absence of major erosional unconformities on the terrace. However, minor exposures of eroded sinter occur between talus cones at the base of the scarp slope to the east of the terrace. Two other sinter deposits outcrop from beneath a thin cover of colluvium along the trace of the South Cross Fault. One lies at the base of the Malpais scarp slope immediately west of the active sinter terrace. The other, exposed in a drill pad cut at the crest of the Malpais scarp above the sinter terrace, lies at the intersection of a N70E-trending fracture and the South Cross Fault (Plate 1).

WHOLE-ROCK CHEMISTRY OF THE MIOCENE VOLCANICS

The major flow units of the Miocene volcanic sequence in the study area have distinctive major element compositional characteristics. These characteristics have proven useful in the discrimination of similar-looking aphanitic flow units for the purposes of mapping and the logging of well cuttings. Table 2 presents whole-rock chemical analyses representative of hand samples and well cuttings from the mapped volcanic units of the study area. Well cutting samples were hand-picked from horizons that appeared fresh in thin section.

The Harker variation diagrams (Figure 4) distinguish three basic rock types within the volcanic pile: a basalt group including samples from the diabase, old basaltic andesite, and late basalt; a basaltic andesite group including samples from the old and young basaltic andesites; and a dacite group including samples from the dacite porphyry and aphanitic dacite of the pyroxene dacite. Each of the plots of the major elements versus SiO_2 produce distinct populations of points. The pyroxene dacite unit contains rocks with high SiO_2 and alkalis, and low MgO, total Fe, and CaO, compared to the basalts and basaltic andesites. The Al_2O_3 content of the pyroxene dacite is generally lower than that of the less siliceous rocks. The alkali content of the dacite declines slightly with decreasing SiO_2, whereas the MgO content increases slightly. Total Fe and CaO contents of the dacite increase more sharply with decreasing SiO_2. The late basalt and young basaltic andesite show similar variability of major elements versus SiO_2, although CaO and MgO increase, and K_2O decreases, more sharply with decreasing SiO_2. The total Fe (FeO) content increases slightly from the young basaltic andesite to the late basalt. The old basaltic andesite and diabase sample have similar major element contents and show similar variability of these elements with silica. However, flows of the old basaltic andesite appear to have a wider range of SiO_2 contents. The analyses produce similar groupings on an AFM diagram as shown in Figure 5.

Figure 6 depicts the variation of the Differentiation Index (DI) with elevation relative to the top of the pyroxene dacite unit. Analyses below the datum are from cuttings of the Ginn well. The first four analyses, above the datum, represent a sequence of young basaltic andesite flows that overlie the dacite aphanitic on the Argenta Rim in the SE 1/4, section 17, T31N, R47E.

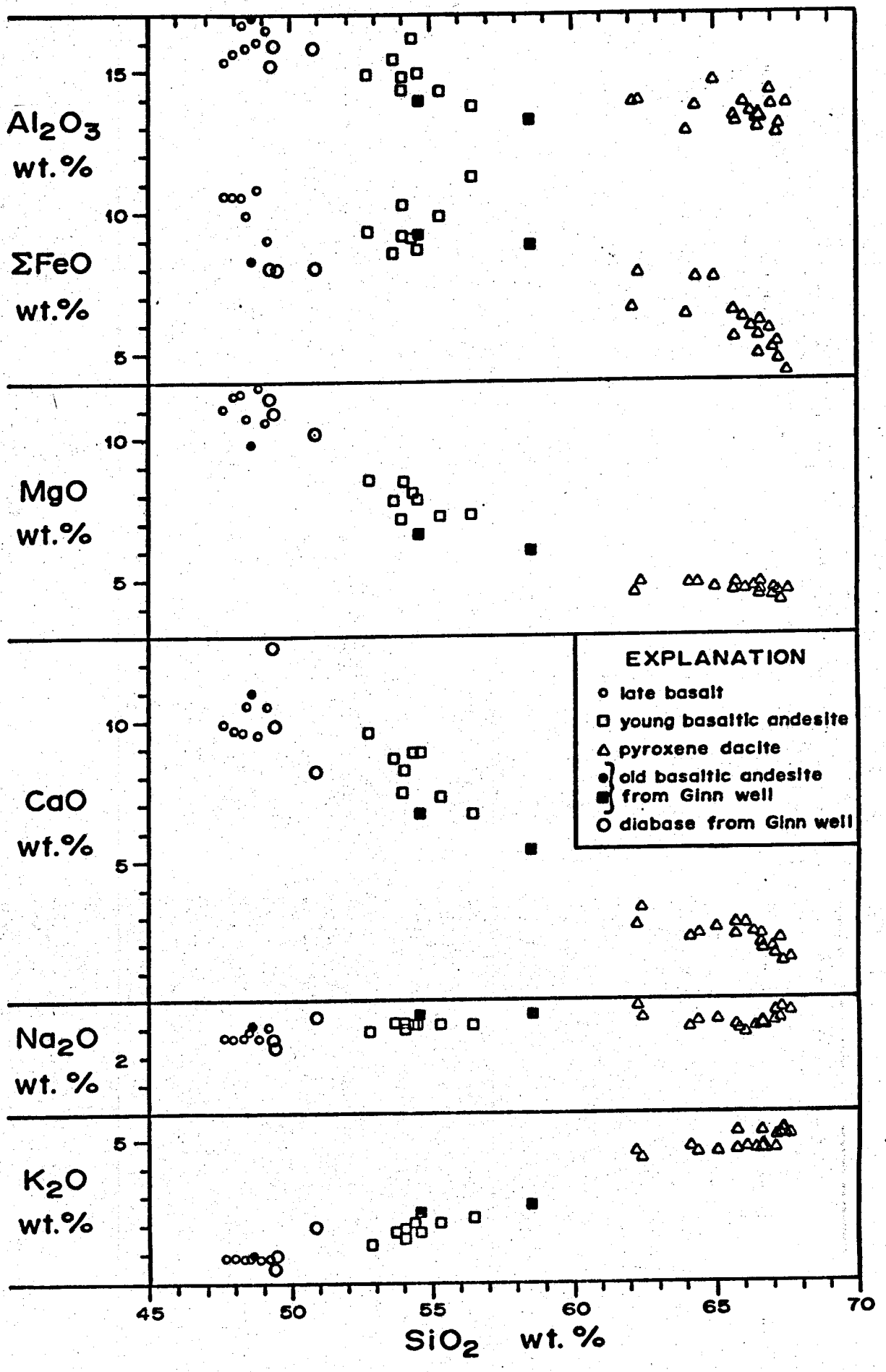

FIGURE 4 HARKER DIAGRAM FOR THE MIOCENE VOLCANICS

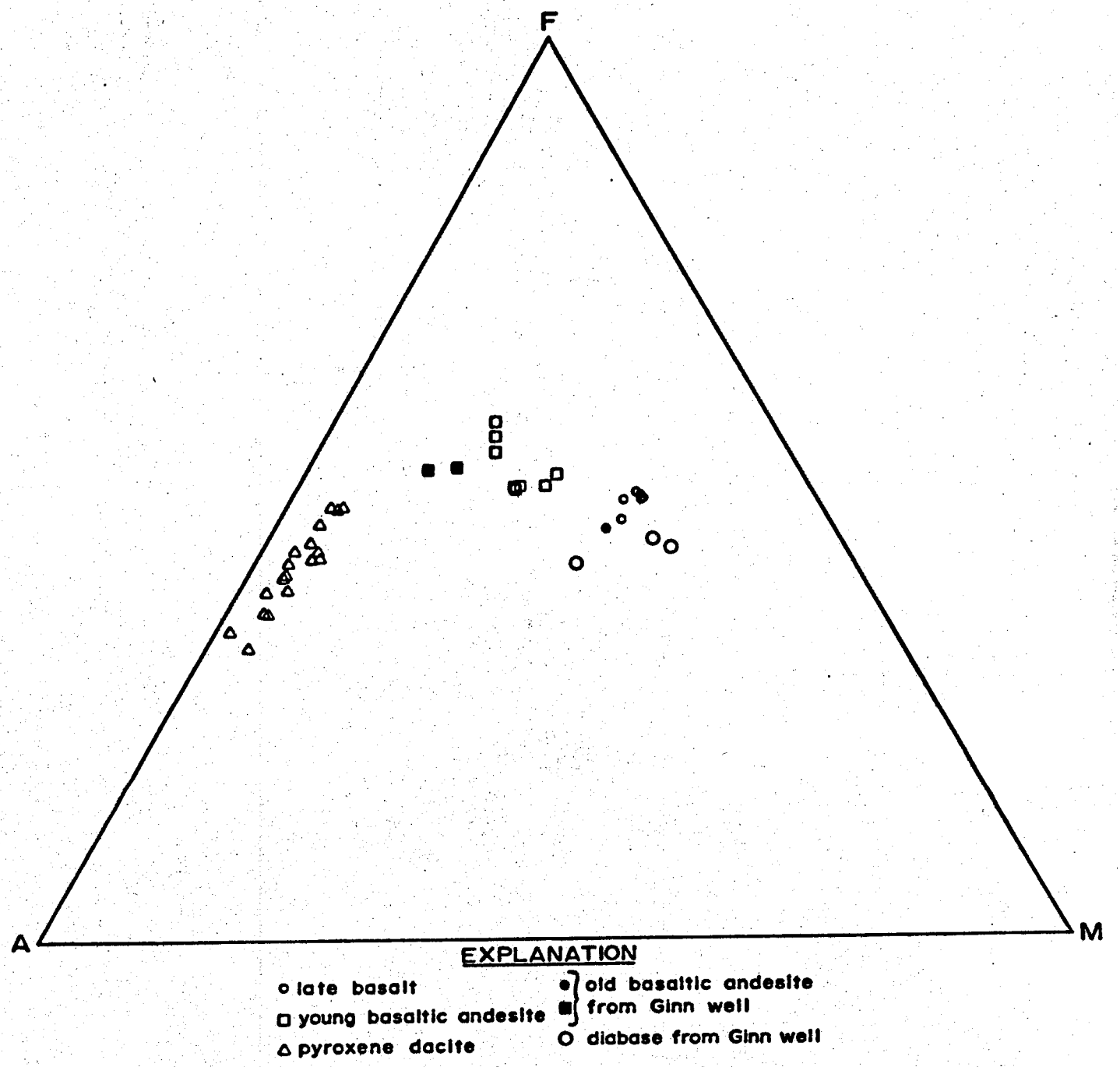

FIGURE 5 A-F-M PLOT FOR THE MIOCENE VOLCANICS

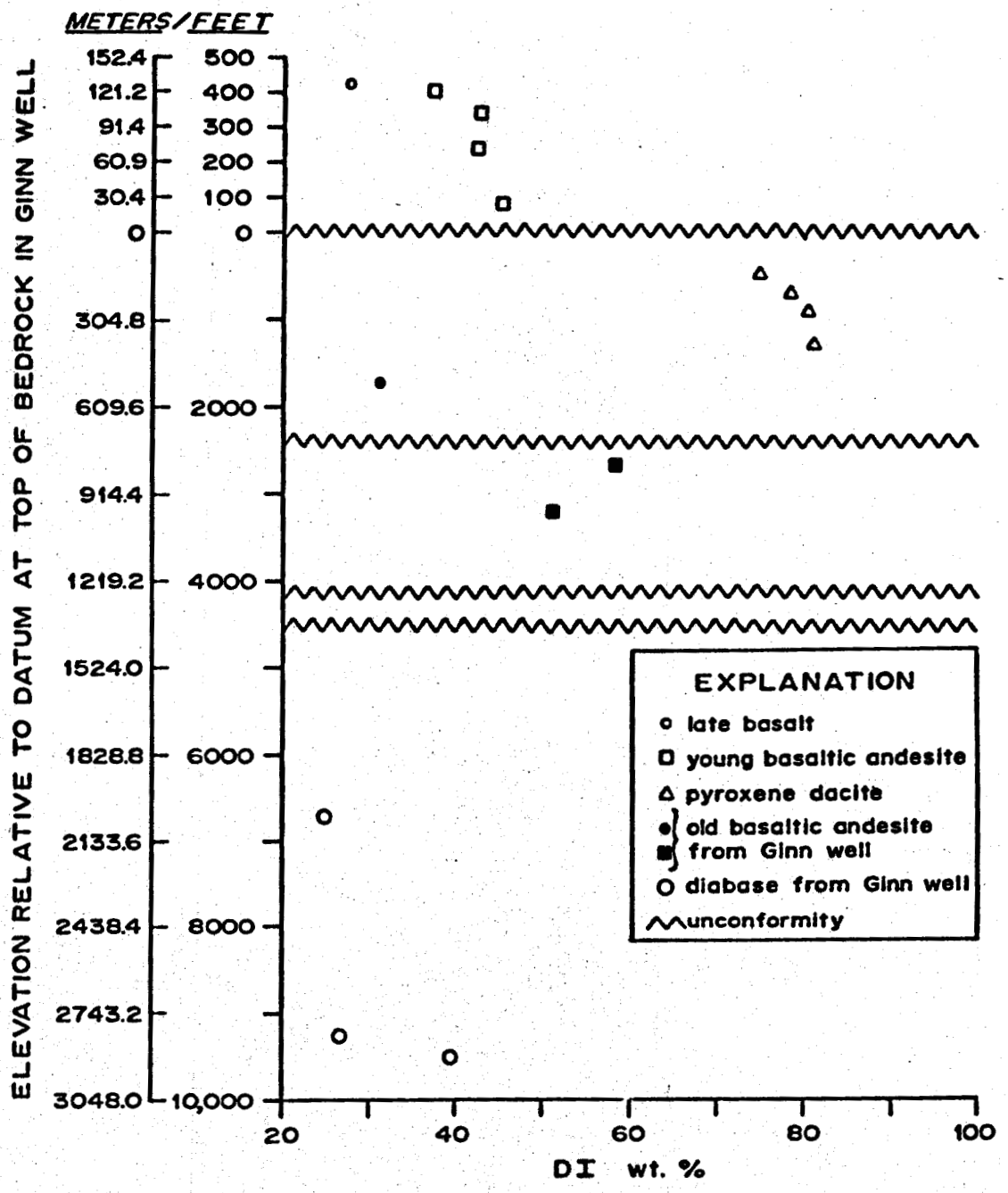

FIGURE 6 ELEVATION VS. DIFFERENTIATION INDEX (DI) FOR THE MIOCENE VOLCANICS

The fifth analysis is an example of the late basalt flows that conformably overlie the young basaltic andesite on portions of the Argenta dip slope. Figure 6 indicates that three cyclical compositional changes occurred during the eruption of the volcanic pile. The limited data suggest that the old basaltic andesite becomes more siliceous upward to the tuffaceous horizons that occupy an erosional unconformity between 610 and 732 m. The basalt flows lying above the tuffaceous horizons may represent the beginning of a new cycle of volcanism. The more siliceous pyroxene dacite probably formed later in this cycle.

Outcrop data substantiate the slight decrease in DI values with depth indicated by the analyses of the Ginn well samples in Figure 6. The decrease of DI values represents the decrease in SiO_2 content of the dacite vitrophyre relative to the dacite porphyry. The young basaltic andesite unit, lying unconformably on the pyroxene dacite, shows a similar decrease in DI values, though the DI values are distinctly lower than those of the pyroxene dacite. The late basalt continues the trend of decreasing DI and represents the termination of basaltic-andesite volcanism at this locality. The basalt lies conformably on the young basaltic andesite, where present, and is slightly younger. The total alkali to SiO_2 diagram in Figure 7 indicates that the Miocene lava flows and dikes at Beowawe plot within the fields of alkalic and high alumina basalt parentage identified by Kuno (1969).

STRUCTURE

Pre-Tertiary Structure

Gilluly and Gates (1965) mapped numerous Paleozoic thrust sheets in the

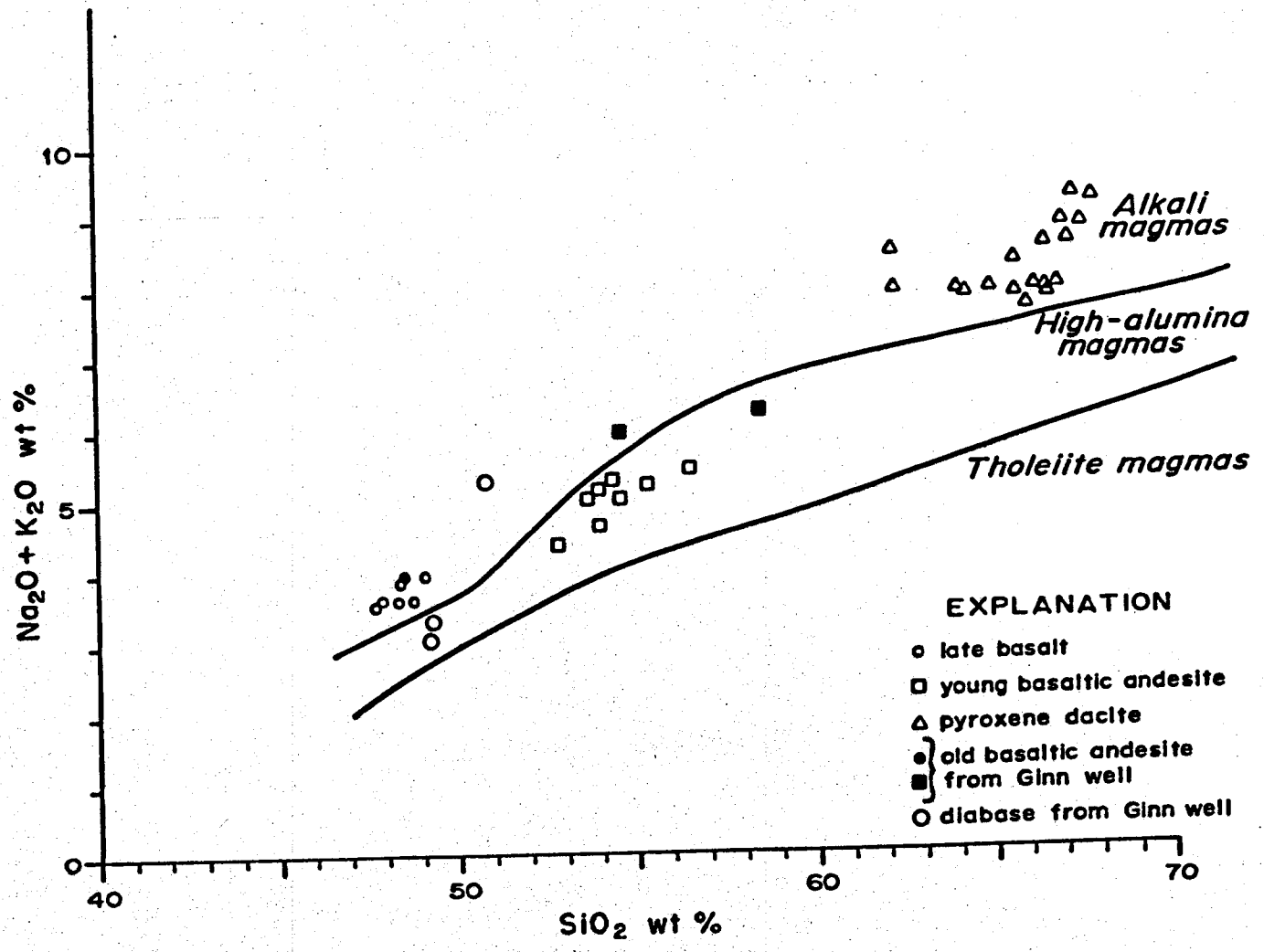

FIGURE 7 TOTAL ALKALIS VS. SiO_2 PLOT FOR THE MIOCENE VOLCANICS; MAGMA TYPE FIELD BOUNDARIES FROM KUNO (1969).

Crescent Valley quadrangle. Stewart and others (1977) extended map coverage of this structural terrain to the north on the west flank of the Argenta Rim. The outcrops of the Valmy Formation on the scarp slope of the Malpais Rim provide a glimpse of the structural chaos exposed in these areas (Plate 1). Pods and horizons of fault breccia are common and often stand in relief at the surface due to silicification. Fault contacts between lithologic horizons are common. The dips and strikes of the bedding units are highly irregular due to the abundance of fractures and tight drag folds. All of the various rock types are thoroughly shattered. The exposures of the Malpais Rim and the fractured nature of the rocks sampled in the deep Chevron wells (Chevron, 1979) indicate that this structural terrain persists at depth beneath Whirlwind Valley (Smith and others, 1979) but do not provide firm evidence for the local depth and orientation of the Roberts Mountain thrust or other major thrust features. The Ginn well does not penetrate the thrust, thereby establishing a minimum depth of 2915 m for the structure. The potentially great thickness of the thrust plate permits an additional 1 or 2 km of depth to the thrust horizon. The Roberts Mountain thrust horizon appears to be significantly depressed in the Whirlwind Valley area relative to the windows exposing the thrust in the surrounding ranges. These windows occur in the Tuscarora Mountains to the northeast, the Pinyon Range to the east, the Cortez Mountains to the south, and the Shoshone Range to the southwest (Stewart and Carlson, 1976).

Tertiary Structure

The Miocene northern Nevada rift has profoundly controlled the development of the structural setting of the Beowawe geothermal area. Zoback

(1978, 1979) described the major structural elements of the rift and applied her regional model to the local structure of the geothermal area. Our mapping effort substantiates and refines her generalized structural models.

Normal faults have produced the topography and post-Oligocene geologic environment of the Beowawe area. Two major fault sets control local geology and topography (Figure 8 and Plate 1): a N50-70°E trend that has produced the Malpais and Argenta Rims, and an orthogonal N15-35°W trend that controls spurs and canyons on the two cuestas (Zoback, 1979). Two additional fault sets have influenced the location and evolution of the hydrothermal system at Beowawe. Elements of a N40-70W trend appear to restrict the outflow of hydrothermal fluid laterally along the Malpais scarp (Oesterling, 1962). A N80-90E fracture set has localized hydrothermal activity in the past and contributed to the structural development of the Whirlwind Valley (Zoback, 1979; Smith and others, 1979).

The Malpais and Argenta scarps define the N50-70E fault trend in the Whirlwind Valley area. Two cuspate flexures divide the Malpais scarp into three segments: the east-northeast Horse Heaven segment, an intervening concave segment, and the east-northeast segment between The Geysers and Beowawe Station (Figure 8 and Plate 1). Faults controlling the latter two segments are called the Malpais fault zone in this report. The Malpais Rim forms the southern margin of Horse Heaven and marks the northeastward extension of the Corral Canyon Fault mapped by Gilluly and Gates (1965) in the Crescent Valley quadrangle to the south. Dip-slip offset, down to the north-northwest, diminishes eastward from a maximum of 500 m in Horse Heaven

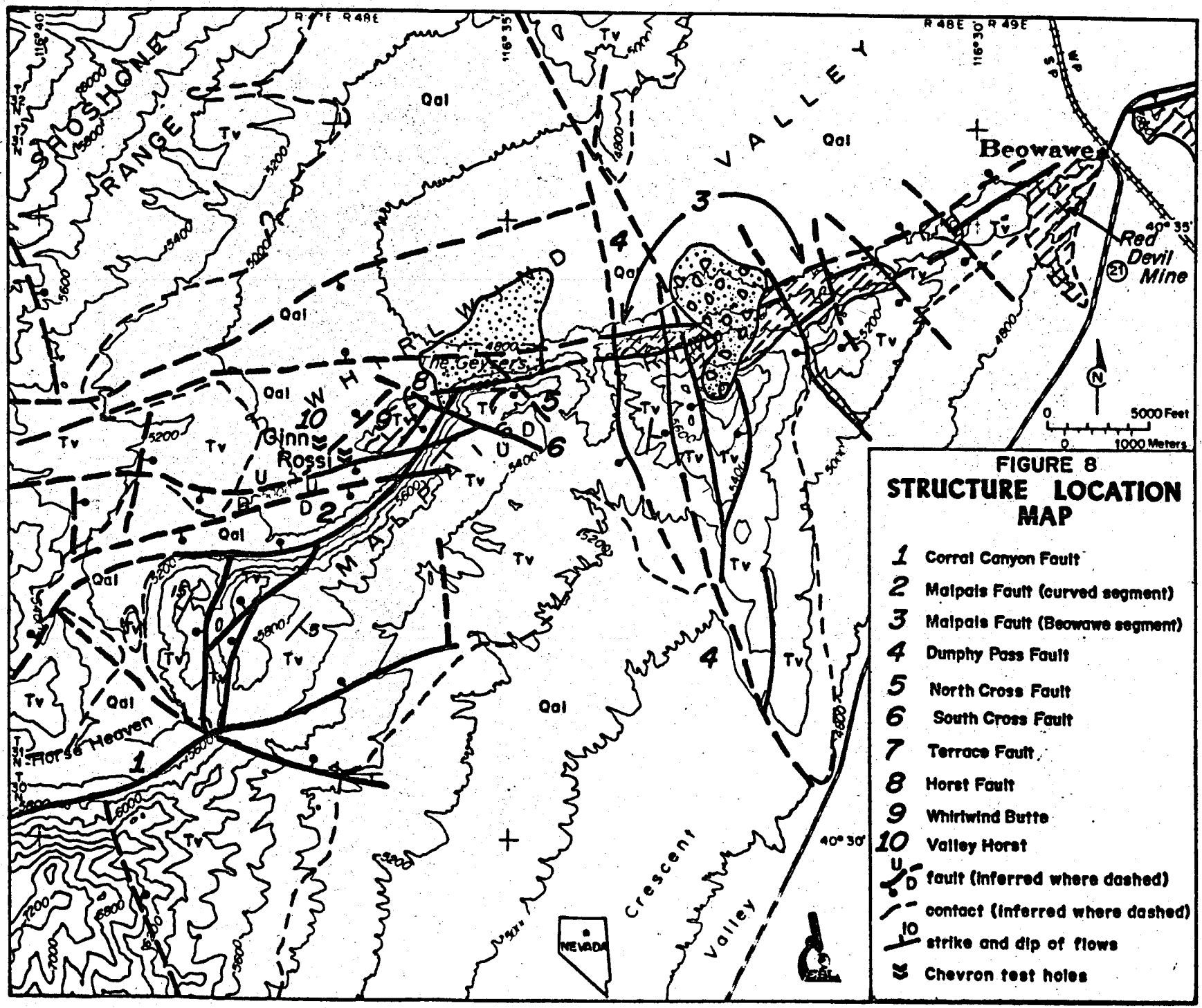
SHOSHONE RANGE
VALLEY
Beowawe
Red Devil Mine
The Geysers
Ginn
Rossi
Heaven
Crescent Valley
NEVADA
Qal
Tv
Ts
R 47 E R 48E
R 48E R 49E
116° 40'
116° 35'
116° 30'
40° 35'
40° 30'
0 5000 Feet
0 1000 Meters
FIGURE 8
STRUCTURE LOCATION MAP
1 Corral Canyon Fault
2 Malpais Fault (curved segment)
3 Malpais Fault (Beowawe segment)
4 Dunphy Pass Fault
5 North Cross Fault
6 South Cross Fault
7 Terrace Fault
8 Horst Fault
9 Whirlwind Butte
10 Valley Horst
U D fault (inferred where dashed)
contact (inferred where dashed)
10 strike and dip of flows
Chevron test holes

to 0 m, as the Corral Canyon fault terminates in the dip slope of the Malpais scarp, south of The Geysers. One major fault with 300 m of offset and at least two faults of minor displacements (<100 m) branch northward from the Corral Canyon fault to the flexure at the mouth of Horse Heaven.

The concave segment, between The Geysers and Horse Heaven, renews the east-northeast trend of the Corral Canyon fault en echelon fashion, but deviates to the northeast, forming a flexure in the Malpais Rim at The Geysers (Figure 8, Plate 1). Maximum dip-slip displacement on this segment is approximately 400 m as indicated by the elevation of the basalt cap unit cut by thermal gradient holes in the valley (Chevron, 1980). A parallel subsidiary fault probably forms the northwestern structural boundary of the fault block that forms the hill southwest of the sinter terrace in Section 18. The hill is called Whirlwind Butte for the purposes of this report. Lithologies observed in several thermal gradient holes (Chevron, 1980) indicate a maximum dip-slip offset of 60 m. Cross faults appear to terminate this subsidiary fault with about 90 m of offset at each end of the butte. Oesterling (1962) mapped an antithetic fault on the southeast side of the butte, which drops a small wedge about 90 m between the Malpais scarp and the butte. He called this the Horst Fault.

The Beowawe segment of the Malpais scarp is an additional en echelon element of the Corral Canyon fault trend (Figure 8, Plate 1). The fault drops the White Canyon tuffaceous sedimentary rocks about 210 m into Whirlwind Valley immediately north of White Canyon, as evidenced by lithologic data from a thermal gradient hole (Chevron, 1980). The minimum possible dip-slip offset

on the Beowawe segment is approximately 150 m in the vicinity of the barite mine. The scarp slope reveals the Ordovician Valmy formation beneath thin layers of the old tuffaceous sedimentary rocks, dacite, White Canyon tuffaceous sedimentary rocks, and basaltic andesite.

The Terrace Fault, identified by Oesterling (1962), traverses the uphill edge of the sinter terrace and is part of the Beowawe segment. He suggested that the Terrace Fault and a possible northeastward extension of the Horst Fault serve as the near-surface conduits for thermal fluids within the Beowawe segment of the Malpais scarp.

The N50-70E-trending faults have tilted the lava flows of the Malpais and Argenta blocks to the south-southeast at dips that range from five to ten degrees depending on the effects of cross faults. The scarp slope is steep with inclinations ranging from thirty degrees on talus and colluvium to vertical on exposed flows. The steep scarp slope profile suggests that the main fault zone is near vertical at shallow depths (Plate II). Electrical resistivity modeling by Smith (1979) supports this proposed fault geometry and extends the near-vertical fault plane to depths in excess of 900 m. A fracture zone, penetrated by the Ginn well at about 2850 m of depth, may be the Malpais scarp fault indicating a decrease in the dip of the fault plane with depth (Chevron, 1979). However, this fracture zone may be subsidiary to the main fault.

The N15-35W fault trend formed a major graben during the late Tertiary although its effect on the local topography is presently more subtle than that of the N50-70E trend. Satellite imagery reveals a strong north-northwest-

trending topographic lineament that transects the Malpais Rim between White Canyon and the young landslide, continues into the Argenta Rim along a low topographic spur, and ends in Dunphy Pass (Garbrecht, 1978). The Malpais scarp slope, immediately east of White Canyon, reveals the juxtaposition of Valmy quartzite and siltstone against aphanitic and porphyritic dacite along north-northwest-trending fractures. The N15-35W fault trend, in White Canyon and on the Malpais dip slope, forms a horsetail pattern on the map (Plate 1). These faults produced dip-slip motion to the west-southwest. We refer to this fracture set as the Dunphy Pass Fault Zone (replaces the name Whirlwind-Crescent Fault in Smith and others, 1979 [Figure 8]). Lithologies encountered in the Ginn and Rossi wells (Chevron, 1979; Smith and others, 1979) and in the Batz well (Zoback, 1979) indicate that as much as 1200 m of Miocene volcanics and younger alluvium accumulated within a developing graben bounded on the east by the Dunphy Pass Fault. Additional northwest-trending faults cut the Malpais scarp immediately west and east of White Canyon though displacements on these fractures are small.

The N25W-trending fault, marking the western limit of the dacite porphyry in Horse Heaven, appears to have been the western margin of the Miocene graben. The exposed thickness of the dacite porphyry, in juxtaposition with the early basaltic andesite unit, suggests a minimum displacement of 240 m down to the northeast. Other lesser faults of this orientation cut the Horse Heaven segment of the Malpais scarp. The basaltic andesite cap flows and minor north-northwest-trending normal faults on the dip slope of the Argenta Rim generally obscure the northward continuation of the western graben margin. However, deep gullying in the northwest quarter of section 15, T31N, R47E

exposes dacite porphyry and, probably, the trace of the graben margin fault. This fault extends to the Argenta Rim at the head of Water Canyon (Figure 1) and, perhaps, influenced the entrenchment of that canyon in the Argenta scarp slope. Renewal of activity on the western graben margin has been slight, but the minor normal faults of the Argenta dip slope may have inherited their orientations from the underlying graben structure.

The N40-70W fault set cuts the Malpais Rim at The Geysers flexure. The most prominent of these fractures confines the surficial geothermal features on the southwest. Oesterling (1962) called this fracture the South Cross Fault (Figure 8, Plate 1). This fault cuts the Malpais dip slope and crest on a slightly curving N60-70W trend and transects the northeast end of Whirlwind Butte immediately west of the sinter terrace. The South Cross Fault has dropped the northeast end of the butte 90 m rotating the flows 25 to 30 degrees to the north. The fault enters the Malpais scarp slope to the southeast and continues to the west edge of White Canyon. Vertical offset on the fault between the scarp crest and the canyon does not exceed three meters. The South Cross Fault probably terminates the Terrace Fault.

The North Cross Fault (Oesterling, 1962) terminates the succession of young thermal vents at the east end of the sinter terrace (Figure 8, Plate 1). The fault strikes about N45W and drops the dacite vitrophyre to the northeast 90 m into juxtaposition with the dacite porphyry. Two additional fractures of similar orientation, though of lesser displacement, cut the Malpais scarp slope on either side of the North Cross Fault.

The N80-90E faults comprise a set of fractures with minor displacements

that diverge slightly from the general Malpais scarp trend. Chalcedony veins occupy numerous fractures of this orientation at the mouth of White Canyon. This portion of the Malpais scarp slope aligns with the veins. The dips of the exposed veins range from eighty degrees north to eighty degrees south due to the rotation of fault blocks on the scarp slope. The east-northeast-trending extension of the Terrace Fault appears to truncate the chalcedony veins. The resistivity modeling and shallow seismic reflection interpretation of Smith and others (1979) and Smith (1979) suggest that these fractures continue westward through the Whirlwind Valley, forming the northern edge of a subtle east-west oriented horst to be referred to as the Valley Horst. The horst exposes the basalt cap unit and underlying dacite vitrophyre on the western floor of the valley. The fault set then develops a splay that breaks the crest and dip slope of the Argenta scarp into several blocks. Shallow seismic reflection data suggest displacements ranging from 30-60 m, down to the north (Smith and others, 1979; Smith, 1979). Another E-W trending fracture appears to traverse the northern edge of Whirlwind Butte, complementing offset on the South Cross Fault, to produce a 100 m-deep alluvium-filled depression revealed by a Chevron (1980) thermal gradient hole.

Six vertical fractures oriented N80-90E cross the crest of the Malpais Rim south and southwest of the sinter terrace. These fractures also transect Whirlwind Butte fault block, where they have been displaced about 100 m to the north by the valleyward movement of that block. Vertical displacements on these fractures do not exceed 20 m where exposed in the Malpais Rim.

Fault patterns and horizontal slickenslides on fault surfaces suggest the

possibility of lateral offset on faults in the study area. Zoback (1978, 1979) emphasizes the significance of lateral offset on fractures of the northern Nevada rift that are oblique to the modern west-northwest direction of least principal regional stress. She maintains that the north-northwest fractures parallel to the rift exhibit right-lateral components of displacement and that east-northeast fractures exhibit left-lateral components of displacement. Left-lateral offset of segments of the linear aeromagnetic high of the Oregon-Nevada Lineament, supported by observed slickensides on faults of the northern Nevada graben and the orthogonal cuestas, provided evidence for her hypothesis. However, our evidence is insufficient to confirm the occurrence of lateral components of displacement on faults in the study area.

Evidence for recent movement on faults in the Beowawe geothermal area is limited. Oesterling (1962) described a 15 m-high scarp, possibly related to earthquakes, along the Terrace Fault. The fracturing displaced sinter and exposed an area of intensely argillized dacite porphyry bedrock and colluvium on the scarp slope above the sinter terrace. The North and South Cross Fractures limit the lateral extent of this fresh scarp. However, this fracture may represent slumping of the sinter terrace due to saturation of the sinter and the highly altered colluvium and bedrock. A faint remnant of a young scarp extends 0.5 kilometers east of the active sinter terrace on the uphill side of patches of older sinter (Plate 1). Fresh scarps do not appear elsewhere along the southern margin of Whirlwind Valley, although the Malpais scarp slope between the terrace and the Quaternary landslide preserves youthful triangular facets. The steep slopes and cliffs of the concave scarp

segment indicate recent and rapid uplift of competent rocks. Parallel retreat of the Malpais scarp slope has been negligible. A subdued scarp extends along the eastern half of the trace of the Corral Canyon Fault on the southern margin of Horse Heaven (Plate 1). The scarp appears to have suffered considerable mass wasting. This feature does not cross the large slump blocks on the southwest end of the Malpais scarp slope. A youthful scarp truncating the alluvial fan on the northside of the Horse Heaven flexure may well be a product of lateral erosion during severe flash flood conditions in the Horse Heaven drainage, rather than of recent faulting.

Numerous young scarps occur in the region surrounding the Beowawe geothermal area (Stewart and others, 1977; Wallace, 1979). Recent scarps in talus and colluvium appear on the north and west sides of the Argenta Rim. Aerial photos also reveal numerous northerly and northeasterly trending scarps immediately to the west of the Argenta Rim on the floor of the Reese River Valley (Stewart and others, 1977) (Figure 1). East-west-trending scarps parallel the western front of the Shoshone Range to the southwest of the Argenta Rim. These fractures align well with the elements of the N80-90E fault set that transects the Argenta Rim in sections 17 and 29 at the west end of the Whirlwind Valley. Wallace (1979) suggests that these scarps are less than 2000 years old. Wallace (1979) also identifies several scarps of similar age at Boulder Flat northeast of, and on trend with, the Argenta scarp (Figure 1). Table 3 lists these and additional young scarps identified by Wallace (1979). The youthful surficial features and modern regional seismicity (Slemmons and others, 1965) indicate that the northern Shoshone Range is seismically active.

TABLE 3

List of Young Fault Scarps Identified by Wallace (1979) near the Beowawe Geothermal Area

(See Figure 1 for approximate locations)

LOCATION	APPROXIMATE ORIENTATION	AGE YRS
Boulder Flat (northeast of Argenta Rim)	ENE	< 2,000
Lower Reese River Valley (west of Argenta Rim)	N-S, NNE, + ENE	< 2,000
Crescent Fault (northward extension of Cortez Mtns)	NNE	< 2,000
Crescent Fault (southwestward extension of Cortez Mtns)	ENE	< 12,000
Crescent Valley (south of Hot Springs Point)	ENE + NNW	< 12,000
Carico Lake (southwest of Crescent Valley)	NNE	< 12,000
Simpson Park Mtns bounding fault (northwest side)	ENE	< 12,000
Dry Hills bounding fault (northwest side)	ENE - NE	> 12,000
Middle Reese River Valley	NNE	> 12,000
Sulfur Springs Range	N-S	>> 12,000

HYDROTHERMAL ALTERATION

Hydrothermal alteration, in close spacial association with the Malpais Fault, extends from The Geysers to the town of Beowawe (Figure 9). The modern hydrothermal activity, centered on the sinter terrace and a peripheral area of altered outcrop, lies at the western end of this 10 km-long alteration zone (Figure 9). Uplift on the Malpais Fault and erosion have exposed areas of silica veining, argillization, and limonitization on the Malpais scarp slope east of the sinter terrace. The intensity of alteration varies greatly along this portion of the alteration zone, apparently due to the influence of cross fractures and lithologies within the Malpais Fault zone during hydrothermal activity. However, colluvium and landslides obscure portions of the Malpais Fault trace and associated alteration. Our study of the relationships of the alteration to mapped structures and lithologies permits a rough reconstruction of the evolution of hydrothermal activity along the Malpais Fault. The following paragraphs will describe these relationships and distinguish portions of the alteration zone based on structural association.

The Geysers sinter terrace is a product of continuing recent hydrothermal activity. The thickest accumulation of sinter lies along the trace of the Terrace Fault, which controls the location of hot springs and fumaroles on the terrace (Figure 9). The North and South Cross Faults confine the active hot springs, sinter terrace, and related bedrock alteration to a 0.6 km length of the Terrace Fault. The terrace tapers rapidly toward the valley though a thin layer of cemented detrital sinter and extends down the Whirlwind Valley drainage for about 1.5 km. Two linear east-west-trending sinter mounds of low

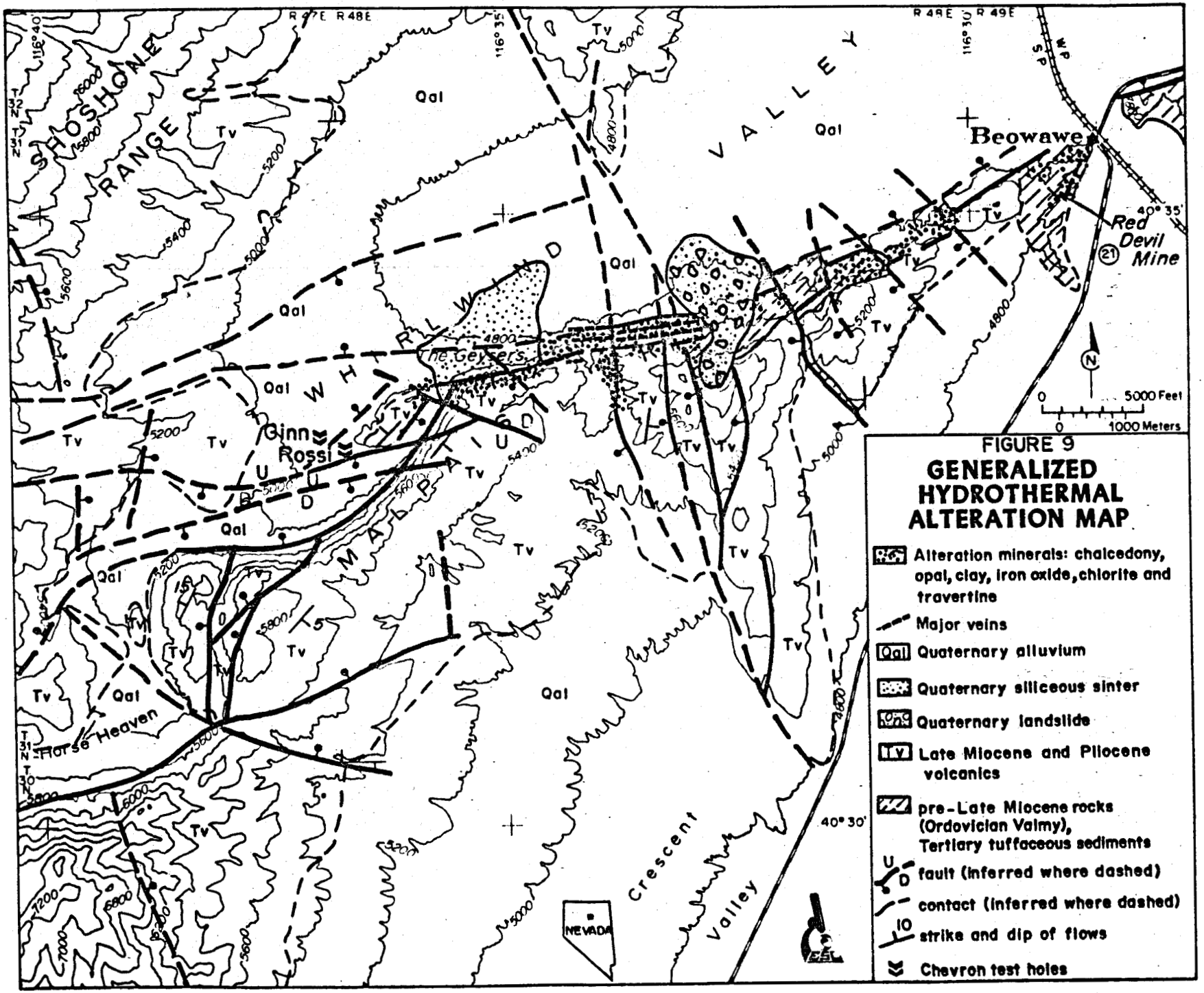
SHOSHONE RANGE
DIXIE VALLEY
WHITE BLUFFS
MADBURY BUTTE
Beowawe
Red Devil Mine
21
The Geysers
Ginn
Rossi
Horse Heaven
Crescent Valley
NEVADA
Qal
Tv
R 47 E
R 48 E
R 49 E
116° 40'
116° 35'
116° 30'
40° 35'
40° 30'
T 32 N
T 31 N
T 30 N
0 5000 Feet
0 1000 Meters
FIGURE 9
GENERALIZED HYDROTHERMAL ALTERATION MAP
Alteration minerals: chalcedony, opal, clay, iron oxide, chlorite and travertine
Major veins
Qal Quaternary alluvium
Quaternary siliceous sinter
Qls Quaternary landslide
Tv Late Miocene and Pliocene volcanics
pre-Late Miocene rocks (Ordovician Valmy), Tertiary tuffaceous sediments
U D fault (inferred where dashed)
contact (inferred where dashed)
10 strike and dip of flows
Chevron test holes

relief lie at the foot of the terrace, one of which appears to have developed from the overflow of several near-boiling springs about 300 m northeast of Whirlwind Butte. The other mound lies 650 m to the north and east of the eastern end of the sinter terrace near the base of the eastern access road. This mound is currently the site of several cool seeps.

Several fractures in the footwall of the Terrace Fault have controlled the circulation of thermal fluids and resultant alteration of the dacite porphyry in the footwall. Excavation of the terrace drill road, during the fall of 1979, revealed open fractures in warm, damp ground. Some of the open fractures contain coatings of white gypsum needles. The dacite is thoroughly argillized to white kaolinite with abundant orange-red to brown limonite on the fractures and altered phenocrysts (Figure 9). Veinlets of opal occupy some fractures. Although the degree of argillization decreases progressively uphill from the terrace, spotty argillic alteration and limonite-coated fractures occur as much as 50 m vertically above the terrace.

The weathered condition and partial burial of the previously described sinter deposits on the trace of the South Cross Fault and on the trace of Malpais Fault, immediately east of the sinter terrace, indicate that they are older than the active terrace (Figure 9). Their ages are uncertain. Altered bedrock lies beneath and peripheral to these deposits. Thin opaline veins up to 5 cm in thickness occupy fractures in dacite porphyry within the trace of South Cross Fault at the base of the Malpais scarp slope. Although colluvium obscures most of the altered rock east of the sinter terrace, patches of limonitized and argillized colluvium at the top of the debris slope mark the

extension of the altered zone to White Canyon. A 30 m-wide zone of strongly argillized and fractured dacite vitrophyre occurs in the access road cut. Orange-red to brown limonite coats fractures. Opal and carbonate veinlets are most abundant at the intersections of the Malpais Fault with northwest-trending cross faults. The previously mentioned patches of sinter and sinter-cemented talus outcrop between debris cones on the lower portions of the scarp slope.

The intersection of the Malpais Fault with the Dunphy Pass Fault zone was the locus of intense hydrothermal activity. Uplift on the Malpais Fault has exposed a dense swarm of east-west-trending chalcedony-carbonate veins cutting dacite porphyry and vitrophyre at the mouth of White Canyon (Figure 9). The chalcedony is banded with occasional carbonate-bearing layers that leave silica pseudomorphs upon weathering. Several large, near-vertical veins of 1 to 2 m in thickness stand in relief over a strike length of about 0.6 km. The Malpais fault truncates the veins to the west at the edge of Whirlwind Valley. The major veins are not traceable to the east of the north-northwest-trending fault contact between the dacite and the Valmy quartzites and siltstones. However, abundant chalcedony veinlets and veins with thicknesses up to 0.3 m continue eastward through the highly fractured Valmy Formation to the young landslide. The abundance of chalcedony veins drops drastically in Valmy exposures to the east of the landslide. The discrimination of post-Miocene silica veins and fault breccias in Valmy outcrops from those attributable to Paleozoic thrust faults is difficult due to the resemblance of the young hydrothermal silica to vein silica in the chert and fractured quartzite horizons of the Valmy. However, continuous east-northeast to east-west-

trending veins and breccia zones are likely to be products of the Malpais Fault and associated hydrothermal activity.

The exposed vein swarm and attendant zone of alteration is 0.2 km wide at an elevation of 1476 m (4920 ft) in the mouth of White Canyon, and extends to an elevation of 1645 m (5400 ft) on the east wall of the canyon. Several thin chalcedony veins, striking N70E, cross the middle of the White Canyon gorge. These veins appear to follow fractures subsidiary to the main Malpais Fault. Chalcedony and opal also fill fractures of the Dunphy Pass Fault zone and open spaces in a subparallel paleo-colluvium or pyroxene dacite flow breccia unit on the eastern wall of White Canyon. This zone extends southward for one km up the canyon between elevations of 1585 m (5200 ft) and 1645 m (5400 ft). The elevation of the top of the alteration zone increases in a step-like manner eastward along the Malpais scarp slope to an altitude of 1700 m (5600 ft) on the west side of the landslide detachment zone. The observed displacements of the alteration zone indicate renewal of motion on the Dunphy Pass Fault zone subsequent to the deposition of the chalcedony veins. The volcanic country rock in the vein swarm is pervasively argillized with thin chalcedony veinlets on fractures. Clays replace both phenocrysts and ground mass with variable intensity increasing toward the silica veins. Our preliminary x-ray diffraction data indicate the presence of both kaolinite and montmorillonite. Abundant red to yellow brown limonite forms films on fractures and replaces disseminated primary magnetite in the groundmass of the volcanic rock. Argillized rock within the most intensely brecciated exposures of the Malpais Fault zone contain disseminated pyrite that weathers to yellow brown and yellow green limonites. Preliminary trace element geochemistry

indicates that these zones contain significant arsenic. Portions of the fault breccia, associated gouge, and country rock are pervasively silicified to jasperoid. The paleo-colluvium, in particular, is thoroughly silicified near the mouth of White Canyon. The unit appears to have been highly permeable, permitting the flow of thermal fluids through open spaces and into the matrix of comminuted country rock and soil. Iron oxides deposited in the matrix give the rock a red, flinty character. Pervasive silicification of this unit extends to the south 0.2 km along the east wall of White Canyon. The older tuffaceous sediment horizon is strongly argillized and occasionally converted to porcellanite where altered. The less reactive Valmy country rock commonly contains red brown limonite on fractures with lesser amounts of clays. Silicification has converted some of the siltstone to porcellanite as well.

Evidence of hydrothermal alteration does not extend along the Malpais Rim southwest of the sinter terrace. Whirlwind Butte exposes hydrothermally altered rock only at its northeastern end. However, several other sites of hydrothermal activity of undetermined association occur in the Beowawe area. A 60 m-long by 3 m-high zone of travertine-cemented dacite porphyry colluvium lies in the steep eastern wall of a gully about 650 m east of the barite-mine in section 12, T31N, R48E. The gully truncates an old slump block and exposes dacite porphyry lying unconformably on the older tuffaceous sediment. The travertine-cemented colluvium occurs at the contact between the two units. The carbonate is massive to bladed in texture. The main Malpais Fault trace probably lies beneath the slump block. There is no evidence for a cross fault at this locality.

At the Red Devil Mine (Figure 1), a N40E-trending vertical fracture zone controls a 30 m-wide fault breccia in Valmy quartzite, siltstone, and chert pebble conglomerate. A northwest-trending cross fault may intersect the northeasterly trending fault at this locality. Silicification has converted large areas of siltstone to porcellanite. The breccia has abundant open spaces and thin zones of mylonite. Quartz-pyrite veins and pyrite films occupy some of the fractures in the breccia zone. Sporadic cinnabar occurs on fracture surfaces. Weathering of the pyrite has produced an abundance of yellow orange to yellow brown limonite in some portions of the breccia. The relative age of this mineralization is uncertain. However, the strong limonitization of the Valmy Formation in the hill directly south of the town of Beowawe seems related to the activity of the Malpais Fault.

Gilluly and Gates (1965) briefly describe a small area of "brightly colored siliceous sinter, opal, and chalcedony and a surrounding zone of much altered lavas" in the Fire Creek drainage five km to the south of Horse Heaven and outside of our mapped area. They do not locate this occurrence precisely, and mention no evidence of recent activity. The Miocene flows offer the only control on the age of this hydrothermal deposit.

The Ginn and Rossi wells penetrate a crudely zoned sequence of hydrothermal alteration products (Figure 3). Our lithologic logs of the well cuttings indicate that the two wells intercepted similar progressions of alteration mineral assemblages at approximately the same depths. The x-ray diffraction data of cuttings from the Ginn well support these observations (Table 4). The shallowest depth at which alteration clearly attributable to

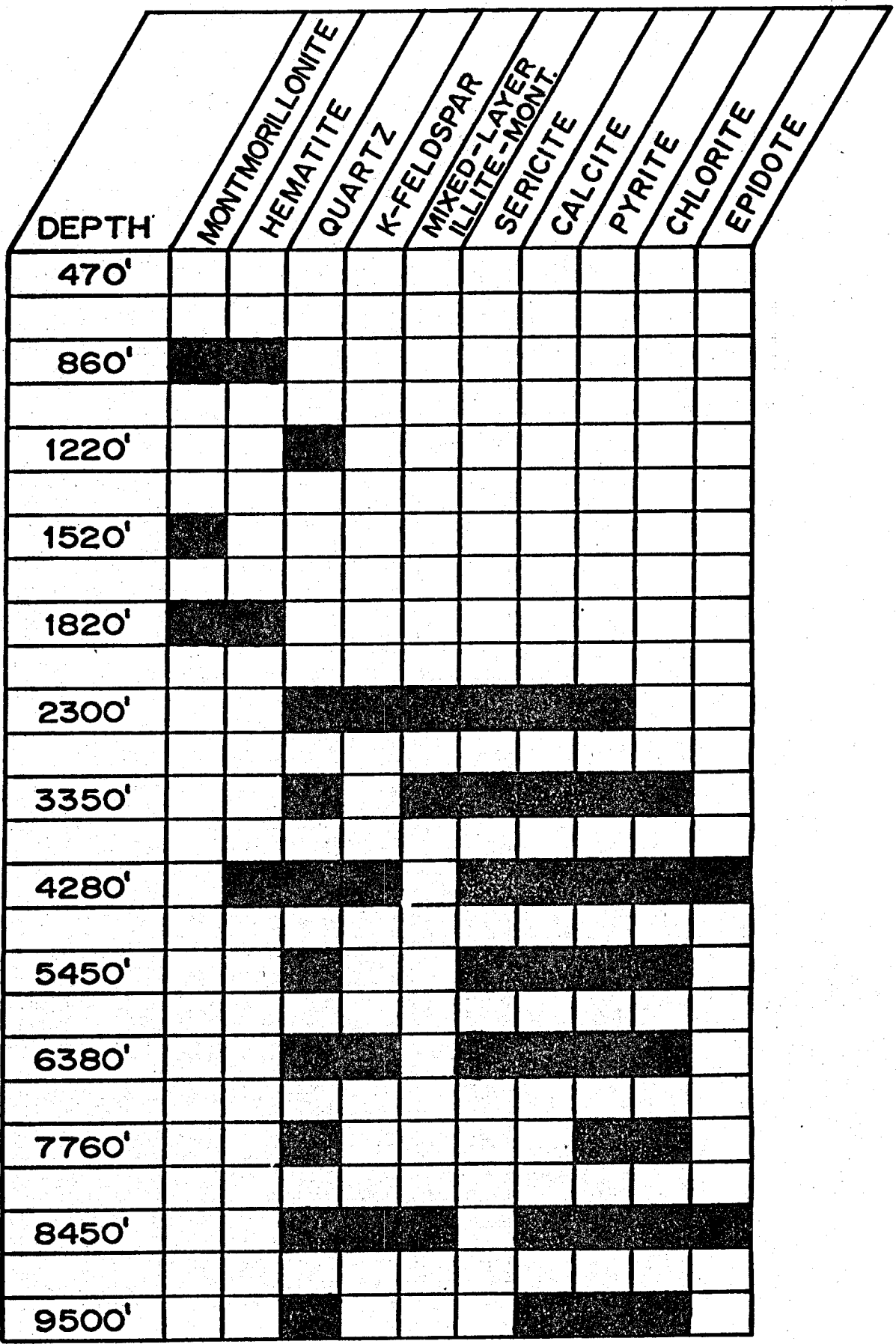

NOTE: K-feldspar above 5450 ft probably primary

Analyst: J. Hulen

TABLE 4 DISTRIBUTION OF ALTERATION MINERALS IN THE GINN 1-13 WELL BASED ON X-RAY DIFFRACTION DATA AND THIN SECTION OBSERVATIONS.

hydrothermal alteration occurs is about 460 m (1500 ft). Above this depth, clays, zeolites, iron oxides, silica, and carbonate occur in the lava flows, but these minerals are not easily distinguished from those of deuteric processes. The shallowest hydrothermal alteration occurs in the old basaltic andesite and appears as the deterioration of plagioclase phenocrysts to calcite and clay and replacement of pyroxene and olivine by clays and minor chlorite. The clays are green or brown and probably belong to the smectite group. Alteration intensifies irregularly over the next 450 m of depth. Mixed-layer clays and chlorite become more common alteration products and epidote appears, occasionally, as grains after plagioclase below 900 m (3000 ft). The shallowest pyrite occurs as abundant disseminated grains in argillized tuffaceous horizons between 628 m (2060 ft) and 747 m (2450 ft). Pyrite persists to greater depths as disseminations and in silica or calcite veinlets. The interbedded older tuffaceous sediment and hornblende andesite units, at a depth of 1220 m (4000 ft), are strongly argillized and contain chlorite and mixed-layer clays after the mafic minerals, and calcite with clays after plagioclase phenocrysts. Some sericite may occur with clays replacing groundmass and plagioclase phenocrysts. Quartz-calcite veinlets and pyrite disseminations are abundant.

The Valmy Formation has a long history of regional metamorphism dating back to the pre-Tertiary orogenies. The products of younger hydrothermal events are superimposed on the metamorphic fabric. The regional metamorphic products are generally fine grained. However, quartz, sericite, chlorite, and possibly actinolite are recognizable in thin section, placing these rocks in the greenschist facies of metamorphism. A weak slaty cleavage distinguishes

metamorphic sericite in the siliceous siltstone. All of the Valmy Formation rocks are brittle and highly fractured. Quartz-pyrite-calcite veinlets are common and locally contain epidote grains. Occasional cavities contain drusy quartz.

The diabasic basalt to basaltic andesite intercepted within the Valmy section ranges from fresh to strongly propyllitized, although all samples observed preserve the diabasic texture of the fresh rock. Calcite, mixed-layer clays, and epidote replace plagioclase, whereas chlorite and clays replace mafic minerals. Quartz-pyrite-calcite veinlets occur, but are less common than in the Valmy Formation. The altered diabase contains finely disseminated pyrite. Paragenetically, quartz and pyrite commonly postdate chlorite and clays in the veinlets and are followed by calcite and clay. This sequence generally persists in both the Miocene and Ordovician sections.

In general, hydrothermal alteration through the Miocene volcanic section changes with depth from a clay-calcite-quartz-pyrite to a chlorite-calcite-clay-quartz-pyrite assemblage. A quartz-calcite-mixed chlorite and clay-pyrite-sericite-epidote assemblage characterize the alteration of all rocks below the Ordovician-Tertiary contact. Tuffaceous horizons reveal a predominant sericite-quartz-clay-calcite-pyrite assemblage. The intensity of hydrothermal alteration is highly variable depending on fracture and lithologic premeability.

Minerals formed by weathering, deuteric alteration, earlier thermal events, and regional metamorphism may confuse the alteration zoning pattern in the drill holes. The epidote of the Miocene volcanic section, in particular,

may be misleading; the early basaltic andesite unit may exhibit propylitization as old as Miocene age. However, epidote grains in quartz-pyrite veinlets are most likely to be related to hydrothermal activity. Pyrite in the volcanics is clearly hydrothermal in origin, but some of the pyrite in the Valmy Formation is probably diagenetic, syngenetic, or metamorphic.

The temperature-depth curve (Figure 10) from the Ginn well (Chevron, 1979) provides evidence for the distribution of hydrothermal fluid flow in the vicinity of the well and the observed zoning of alteration minerals toward higher temperatures of formation with depth. The well penetrates a major fracture zone below 2438 m (8000 ft) and becomes essentially isothermal to total depth with a maximum temperature of 214°C occurring at 2883 m (9460 ft). Chemical geothermometer calculations, as applied to waters of the boiling springs and steam wells at The Geysers, suggest the presence of a reservoir with temperatures of about 225°C (Renner and others, 1972; Mariner and others, 1974; Muffler, 1978; Robinson, 1979). Minor temperature reversals occurring in this interval suggest the presence of cold water entries. The low gradient persists upward to a depth of 1682 m (5520 ft), indicating significant convective heat loss over this interval. The high gradient extending from 1682 m upward to a depth of about 300 m suggests conductive heat loss. The suggested temperature and hydrologic conditions below 1682 m could induce the observed hydrothermal alteration, whereas the absence of fluid at shallower depths precludes the ongoing formation of the alteration minerals observed there. These observations complement petrographic data, suggesting that alteration minerals have reduced the permeability of the rock at shallow

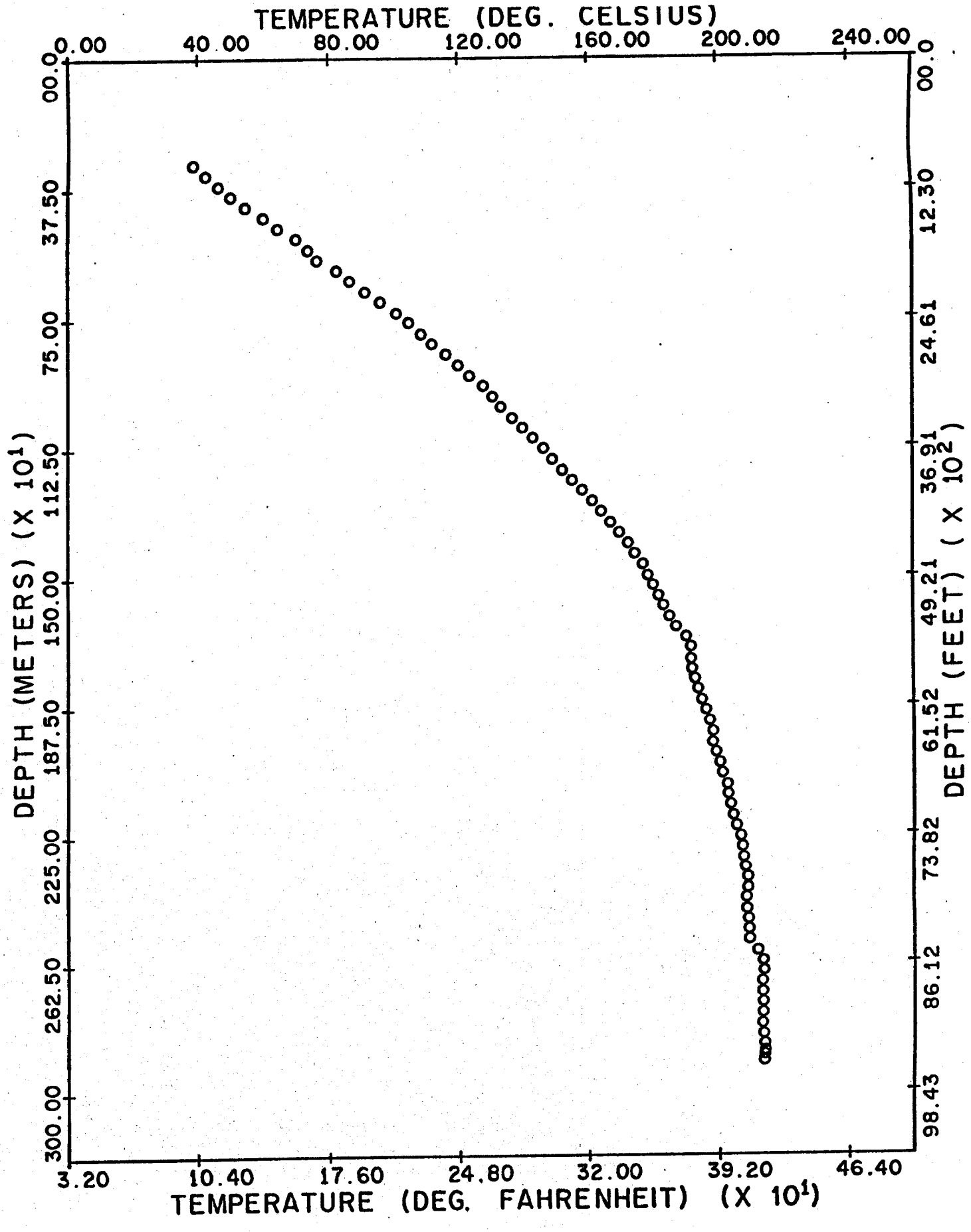

FIGURE 10 TEMPERATURE VS. DEPTH PLOT FOR THE GINN 1-13 WELL; DECEMBER 12, 1974.

depths thereby restricting the flow of the hydrothermal system. The probability of fault-controlled fluid flow suggests that the observed thermal gradients and alteration minerals may depend on the proximity of the well to a fluid-bearing fracture at any given depth rather than the proximity to a heat source at greater depth.

Thermal fluids of the modern hydrothermal system are anomalous in composition compared to other hydrothermal systems of similar temperatures in the Basin and Range. The fluids, with less than 1500 ppm total dissolved solids, have low salinities in spite of their apparently active role in the production of alteration minerals (Table 5). The chlorine content is very low while SiO_2 levels are unusually high.

The compositions of the thermal fluids at Beowawe closely resemble those of the water of the nearby Humboldt River. This evidence, coupled with the short thermal fluids residence time indicated by the low salinities, suggests that the Humboldt River may recharge the Beowawe geothermal system. The low salinities suggest that the modern fluids are not related to the hydrothermal system that produced the strongly mineralized and altered zone in White Canyon.

DISCUSSION OF THE GEOLOGIC HISTORY

The chronology of Tertiary volcanism established by the stratigraphy and ages of the flows permits the reconstruction of the Oligocene to Recent structural history of the Beowawe geothermal area (Figures 11 and 12). The old tuffaceous sedimentary rocks with the intercalated 38.5 $\pm$ 1.3 m.y. old

TABLE 5

Fluid Compositions from the Beowawe Area Hot Springs and Thermal Wells, and the Humboldt River.

(Parts per Million)

	Horse-shoe Ranch	Beowawe Geysers	Beowawe Geysers	Beowawe Geysers	Beowawe Geysers	Hot Springs Point	Vulcan 2A Well	Humboldt River at Beowawe
^{o}F	136.4	204.8	-----	-----	-----	138.2		
^{o}C	58	96	-----	-----	-----	59		
pH	7.0	9.5	-----	-----	-----	6.8		
SiO_2	58	373	449	413	418	72	329	33
Al	-----	.0	0			-----	.2	0
Fe	-----	.04	trace	trace	trace	.04		
Mn	-----	0.0	-----	-----	-----	0.09	trace	
Ca	22	0.8	2	trace	trace	54		50
Mg	5.8	.0	0	0	0	38		13
Ba	-----	-----	-----	-----	-----	-----		
As	-----	-----	0	-----	-----	-----		
Na	136	230	239	216	282	277	214	58
K	17	16	33			51	9	8.5
Li	.0	1.3	-----	-----	-----	1.0	trace	
NH_4	6.4	0.5	4?	-----	-----	-----		
HCO_3	378	116	129	244	512	928	41	256
CO_3	0	149	173	84	trace	0	168	0
SO_4	62	89	97	84	91	116	89	56
Cl	27	30	47	30	70	49	50	30
F	5.0	15	11	-----	-----	6.9	6	.7
Br	-----	0.4	-----	-----	-----	-----		
NO_3	-----	0.4	-----	-----	-----	3.3		2.5
PO_4	-----	-----	-----	-----	-----	0.0		
S_2O_3	-----	-----	1	-----	-----	-----		
B	.81	2.0	?	-----	-----	1.6	1	.3
H_2S	-----	5.5	0	-----	-----	-----	6.1	
Sum, as reported	718.01	1028.94	1192.00	1071.00	1373.00	1373.00		435

TABLE 5 (cont.)

1. Hot spring on Horseshoe Ranch, 1 mi N.E. of Beowawe, Sec. 32, T32N, R49E, collected by D. C. White, analyzed by H.C. Whitehead and J.P. Schluch, U.S.G.S. H_2S estimated in the field, (taken from Roberts et al., 1967).

2. Beowawe Geysers, pool below terrace, Sec. 17, T31N, R48E, collected by D. E. White, analyzed by H.C. Whitehead, U.S.G.S. SiO_2 gravimetric; also reported: Sr. 0 ppm; I, 0.0 ppm, (taken from Roberts, et al., 1967).

3. Beowawe Geysers, small geyser, Sec. 17, T31N, R48E, collected by T. B. Nolan and G. H. Anderson, analyzed by E. T. Allen, Geophysical Laboratory (Nolan and Anderson, 1934, p. 227). B, As, and H_2S reported as B_2O_3, AsO_4, and S. (taken from Roberts, et al., 1967).

4. Beowawe Geysers, hot spring, Sec. 17, T31N, R48E, collected by R. F. Garnett, Beowawe, analyzed by S. C. Dinsmore, Univ. of Nevada (Nolan and Anderson, 1934, p. 227), (taken from Roberts, et al., 1967).

5. Beowawe Geysers, geyser, Sec. 17, T31N, R48E, collected by R. F. Garnett, Beowawe, analyzed by S. C. Dinsmore, Univ. of Nevada (Nolan and Anderson, 1934, p. 227), (taken from Roberts, et al., 1967).

6. Hot Springs Point, Sec. 11, T29N, R48E, collected by G. C. Simmons, analyzed by C. G. Mitchell, U.S.G.S., (taken from Roberts, et al., 1967).

7. Vulcan 2 well, on sinter terrace, Sec. 17, T32N, R48E, Eureka County, NV, analyzed by Abbot A. Hanks, Inc. (Lawrence Berkeley Laboratory, 1977).

8. Humboldt River sampled at Beowawe by the U.S.G.S., analyzed by the U.S.G.S. (Eakin and Lamke, 1966).

hornblende andesite flows accumulated unconformably on the Ordovician Valmy Formation. Evidence for structural control of the thickness and areal distribution of these units is inconclusive. However, the overlying old basaltic andesite accumulated to a thickness of 600 m within a north-northwest- trending graben (Figure 12a). The ages of the old basaltic andesite and the graben are uncertain. An erosional unconformity occurs in the tuff and tuffaceous sediment sequence near the top of the old basaltic andesite. Therefore, the basalt above the tuffs of the old basaltic andesite may be a part of the subsequent pyroxene dacite eruptive sequence.

The 16.1 $\pm$ 0.6 m.y. old pyroxene dacite accumulated within the graben and overflowed the eastern boundary represented by the Dunphy Pass Fault zone (Figure 12b). The White Canyon tuffaceous sedimentary rocks and the young basaltic andesite flows also appear to have overflowed the graben margin toward the east and now appear as the thin cap sequence on the Malpais Rim east of White Canyon (Figure 12, c and d). The unusually thick tuffaceous sediment section in White Canyon apparently accumulated against a topographic high created by the graben boundary fault before overlapping the graben margin. Faulting remained active or resumed on the Dunphy Pass Fault zone after the cessation of volcanism; this accounts for the elevation of the volcanic units, in the east wall of White Canyon, relative to corresponding horizons in the Malpais dip slope to the west. The total vertical displacement of the top of the dacite unit, from the upper floor of White Canyon to its highest exposure on the Malpais Rim, is about 200 m. The White Canyon tuffaceous sedimentary rocks and young basaltic andesite also appear to have overlapped the western graben margin, as evidenced by the presence of

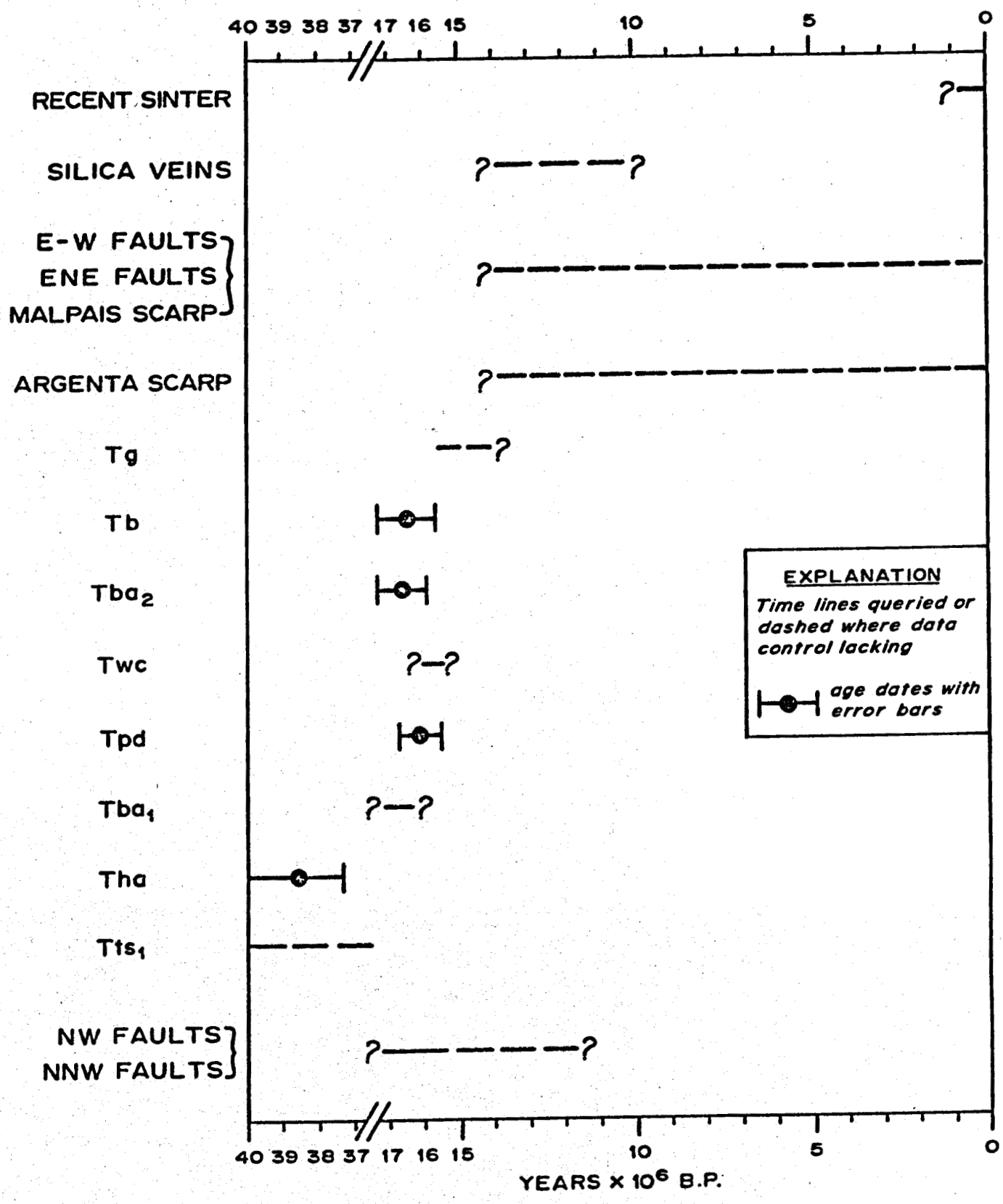

FIGURE 11 SUMMARY CHRONOLOGICAL DIAGRAM OF GEOLOGIC EVENTS WITHIN THE BEOWAWE GEOTHERMAL AREA

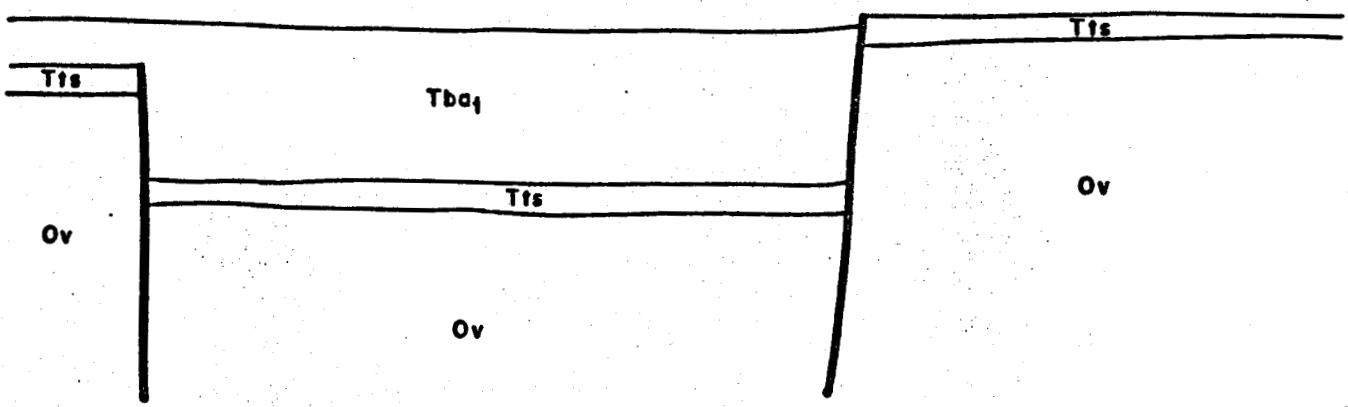

12a INITIAL GRABEN FORMATION AND ERUPTION OF THE OLD BASALTIC ANDESITE

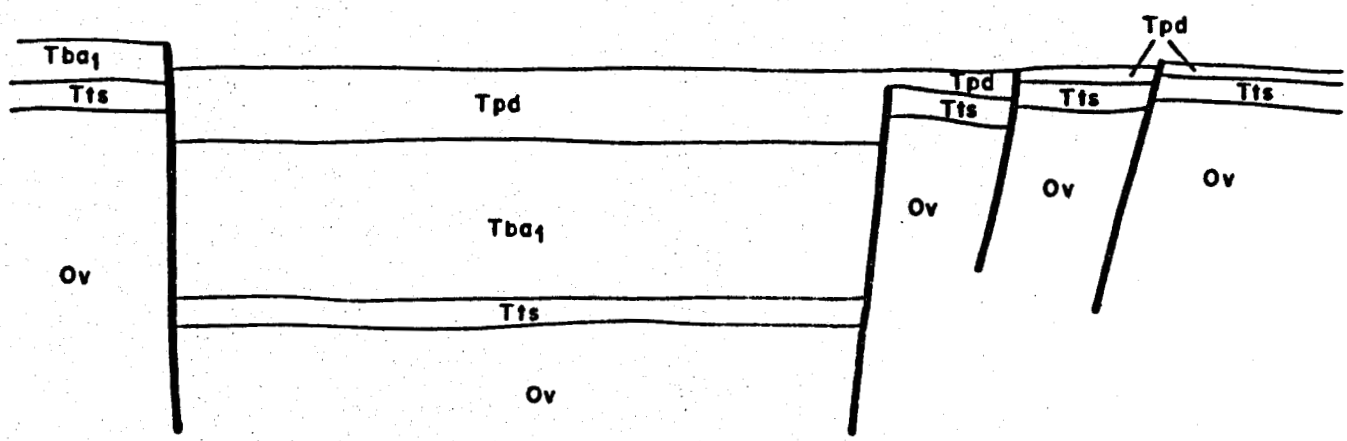

12b ERUPTION OF THE PYROXENE DACITE

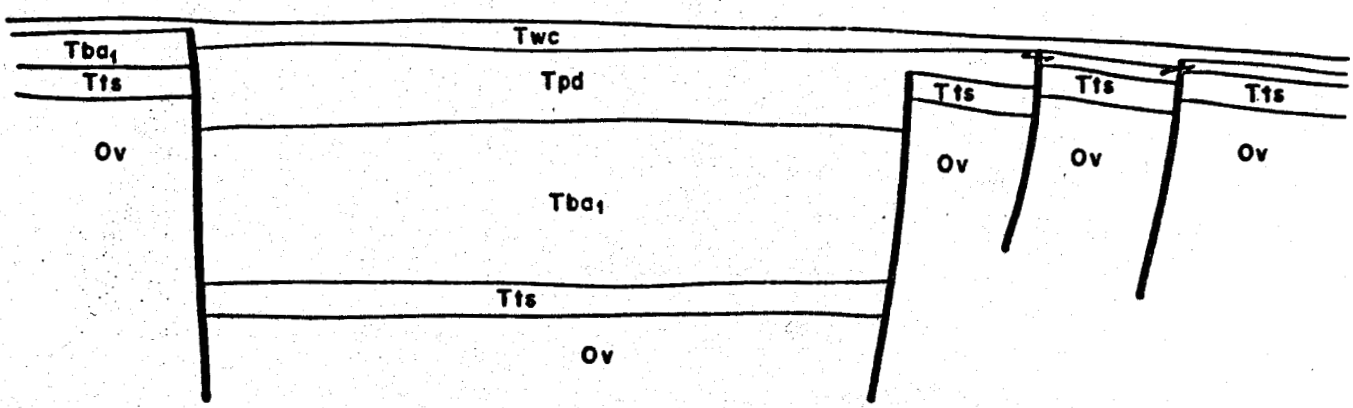

12c DEPOSITION OF THE WHITE CANYON TUFFACEOUS UNIT

FIGURE 12a-e SCHEMATIC RECONSTRUCTION OF THE LATE TERTIARY STRUCTURAL AND VOLCANIC HISTORY OF THE NORTH-NORTHWEST-TRENDING GRABEN.

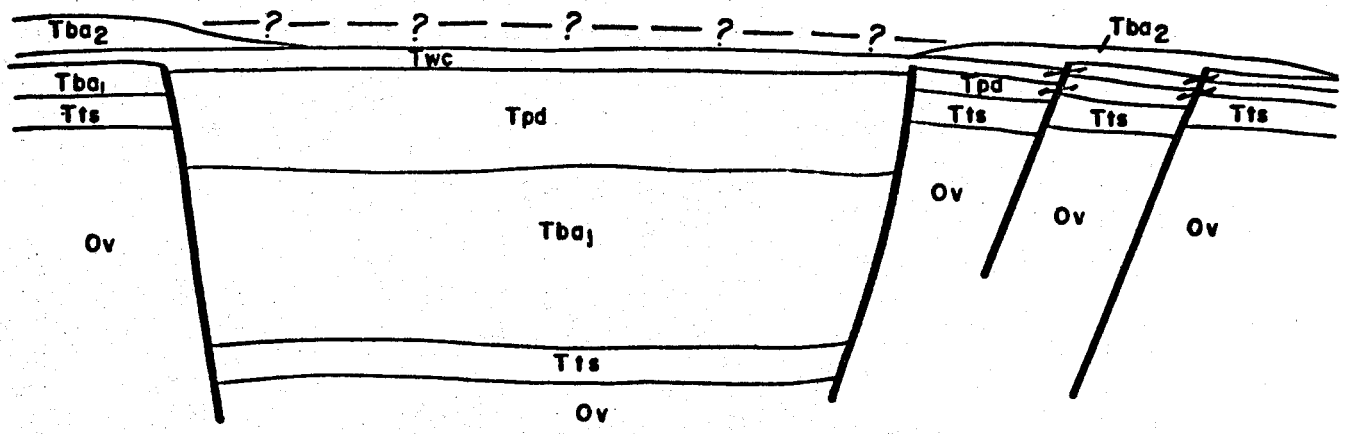

12d ERUPTION OF THE YOUNG BASLTIC ANDESITE

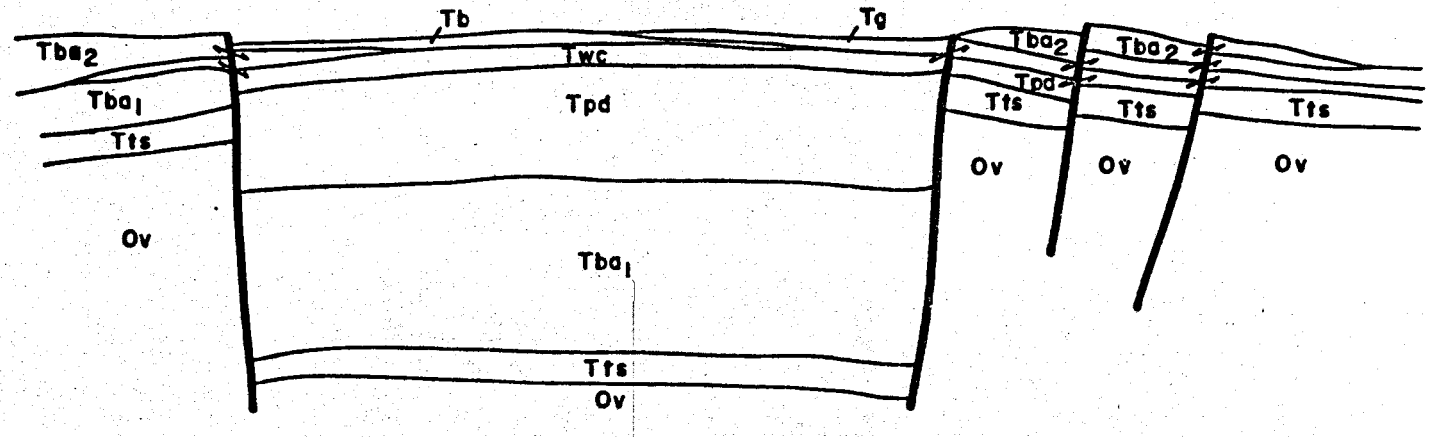

12e ERUPTION OF THE LATE BASALT AND DEPOSITION OF THE TERTIARY GRAVELS

FIGURE 12a-e (continued)

these units on both sides of the boundary fault. Erosion has locally stripped these units from the Malpais dip slope exposing the fault and the pyroxene dacite. The 16.5 $\pm$ 0.7 m.y. old late basalt was the final eruptive product and appears to have remained within the graben boundaries (Figure 12e). Age dates from the Miocene volcanic sequence indicate that the flows above the old basaltic andesite erupted in rapid succession between 15.5 and 16.7 m.y. ago. The graben appears to have deepened as volcanism progressed.

The late Miocene gravel accumulated on the late basalt within the graben (Figure 12e). The east-northeast and east-west-trending faults of the Malpais Fault Zone displace the gravel and all older units. These faults show no evidence of having controlled the deposition of the gravel or any older units, suggesting that fault movements producing the Malpais scarp postdate the deposition of the gravel. The late basalt provides the best constraint on the maximum age of the scarp.

Hydrothermal fluids depositing chalcedony, opal, and minor carbonate circulated within the Malpais Fault and connected portions of the Dunphy Pass Fault. The elevation of segments of major east-west-trending veins and minor north-northwest-trending veins in the Malpais scarp east of White Canyon indicates that the scarp may have grown as much as 180 m since the deposition of the veins. The hydrothermal fluids appear to have invaded and sealed the fractures of the Malpais-Dunphy Pass Fault intersection early in the development of the Malpais scarp. The zone of intense alteration between White Canyon and the sinter terrace has undergone only minor uplift.

Therefore, this alteration zone and the sinter terrace appear to be products of Pleistocene to Recent hydrothermal activity.

CONCLUSION

The observed structures and lithologies coupled with measured fluid temperatures and compositions provide models for the hydrothermal conduits, reservoir, and recharge mechanisms. The following paragraphs will address each of these subjects. Figure 13 illustrates these models.

Shallow Conduits

The intense hydrothermal activity of The Geysers at the structural intersections of the Malpais Fault zone and the North and South Cross Faults indicates that fracture conduits confined to the Malpais Fault zone lie beneath the sinter terrace. The small displacements observed on the cross faults suggest that these fractures and therefore the conduit may not extend to great depth at this locality. East-west-trending fractures may also serve as conduits feeding the hot springs on the flats at the foot of the terrace. However, the Dunphy Pass Fault, as the eastern boundary of the 1500 m (5000 ft) deep northwest-trending graben, must extend to a depth in excess of 3000 m (10,000 ft). Therefore, the intersection of the Malpais and Dunphy Pass Fault zones is the most likely structure to accommodate a deep conduit. Numerical modeling of resistivity data (Smith and others, 1979; Smith, 1979) suggest that a 5 ohm-meter low-resistivity zone exists below a depth of 915 m (3000 ft) at the intersection of the Malpais and Dunphy Pass Fault zones. This zone extends to the west and reaches the surface at the sinter terrace. The zone represents either thermal fluids or conductive alteration minerals from an

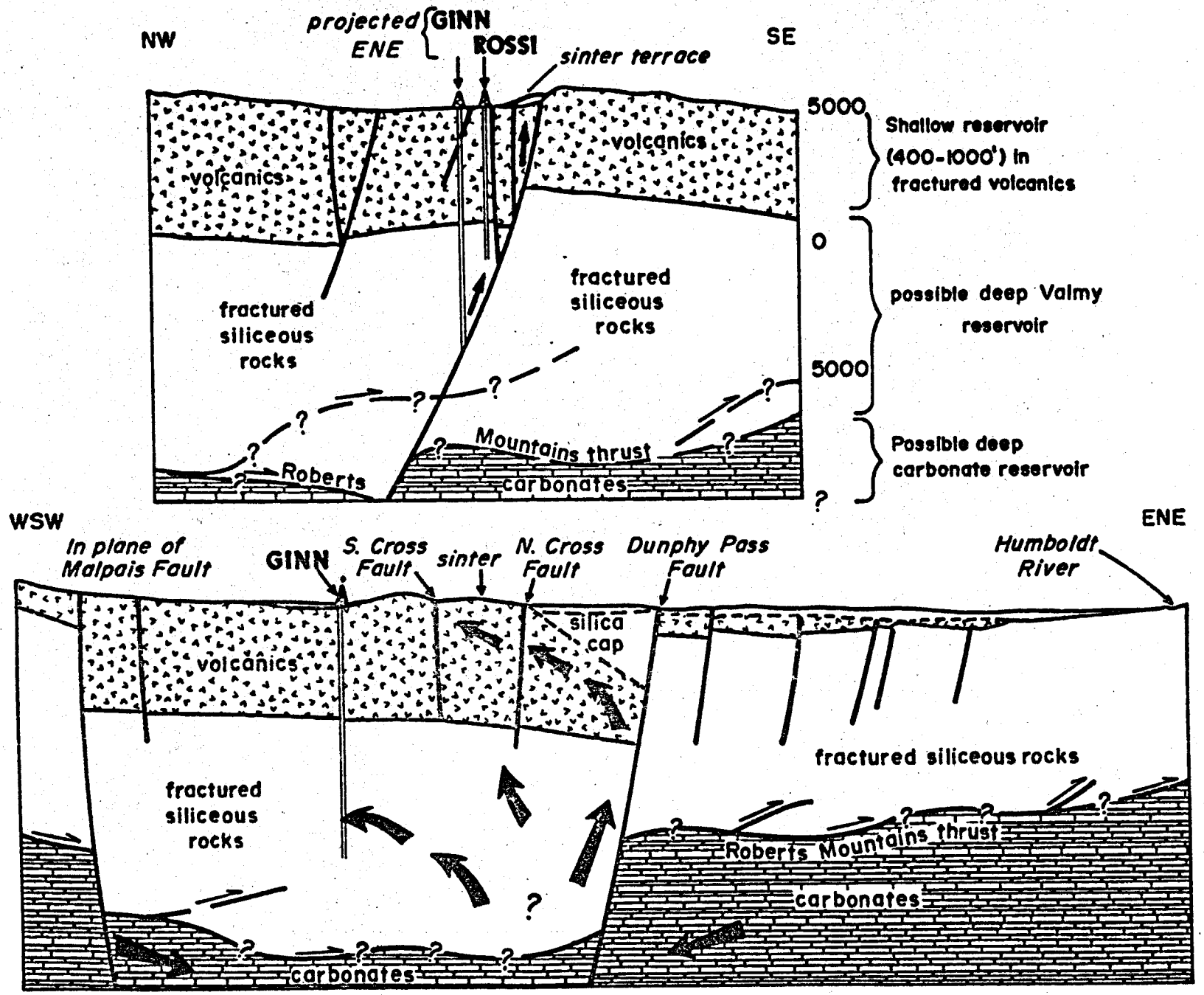

FIGURE 13 BEOWAWE RESERVOIR MODELS

older hydrothermal system. A 300 ohm-meter high resistivity body extends from about 900 m depth to the surface within the fault intersection just east of White Canyon, perhaps representing the silicified zone in Ordovician and Tertiary rocks above the deep conduit. Sealing of the shallow portions of the conduit, suggested by the presence of the vein swarm, may presently divert hydrothermal fluids to the west along the Malpais Fault zone, ultimately producing the sinter terrace above permeable fault intersections. Fault geometries in the vicinity of the Ginn well are also favorable for the westward migration of thermal fluids from the conduit at White Canyon. The Malpais Fault and east-west fractures passing through and north of Whirlwind Butte are probable conduits. However, the existing data do not eliminate the possibility that the intersection of the South Cross and Malpais Faults may be the principal deep conduit.

Reservoir Models

The Beowawe geothermal system appears to sustain shallow and intermediate depth reservoirs at and above the 2915 m depth penetrated by the Ginn well. Temperature data suggests that a deep reservoir may be the source for these reservoirs. The similarity of the measured and calculated temperatures suggest that the waters encountered in the shallow wells and the deep Ginn and Rossi wells are near the deep reservoir temperature. The depth and nature of any deep reservoir is uncertain.

Declining or unreliable fluid production rates encountered after drilling (Oesterling, 1962; Chevron, 1979) suggest that the sealing of the faults and fractures in the country rock may reduce permeability and conserve heat and

fluids in shallow to medium depth reservoirs without rapid recharge. The low thermal conductivity of rocks in the thick Miocene volcanic pile may produce further conservation of heat. These reservoirs probably lie within fractured zones of the Valmy Formation and Miocene lava flows, and within interflow gravel zones. The fractured competent horizons of the Valmy Formation and Miocene lava flows may have locally high permeability, though perhaps low porosity, sustained by tectonic activity along the major faults. Although a thick carbonate sequence capable of sustaining a geothermal aquifer probably exists at depth beneath the Beowawe area (Edmiston, 1979; Zoback, 1979), we find neither geologic nor geochemical evidence to indicate that the Beowawe thermal fluids flow from such a reservoir.

Recharge Models

Fractures due to normal faulting probably carry cold groundwater to depth, supplying a reservoir either within fractured siliceous rocks or carbonates. The nearby Humboldt River is, perhaps, the most reliable water source in the region. Water from the Humboldt River can access the Malpais Fault at the town of Beowawe and the Dunphy Pass Fault on the north side of the Argenta Rim. A playa lake at the mouth of the Whirlwind Valley maintains a static water table at or slightly below the elevation of the Humboldt River just downstream of Beowawe. This static water table extends to the southwest across the trace of the Dunphy Pass Fault zone (Olmstead and Rush, 1975), within Whirlwind Valley, permitting access of cold water to this portion of the fault zone. Fractured Paleozoic siliceous rocks lying beneath the alluvium of the Humboldt River valley between Beowawe and the northeast corner of the Argenta Rim may also carry groundwater to great depths. An alternative

recharge mechanism to be considered is the northward lateral movement of hot fluid from the depths of the Crescent Valley to the Beowawe geothermal area along the southward extension of the Dunphy Pass Fault zone. Hot Springs Point lies on this fault trend. Permeable lithologies may also figure prominantly in this mechanism.

In conclusion, the available data support the fault-controlled recharge of shallow reservoirs within the Micoene volcanics and the fractured siliceous rocks of the upper plate of the Roberts Mountain thrust. The data suggest that these reservoirs derive fluid from an unidentified deep reservoir by means of a conduit at the highly fractured Malpais-Dunphy Pass Fault intersection. Silica has sealed this conduit at shallow depths, possibly causing the locus of modern hydrothermal activity at the surface to occur to the west within the Malpais Fault zone.

ACKNOWLEDGMENTS

I wish to extend my gratitude to M. Lane and J. Iovenitti of Chevron Resources Company and C. Smith of the Earth Science Laboratory for sharing their insight to the geology of the Beowawe geothermal area. Many discussions with J. N. Moore and C. Smith were most beneficial. Critical reviews of the manuscript by J. N. Moore, H. P. Ross, O. D. Christiansen, D. L. Nielson, and P. M. Wright, are greatly appreciated. The drafting was done by Dawnetta Bolaris and Connie Pixton and the typing by Lucy Stout.

Funding was provided by the Department of Energy, Division of Geothermal Energy, to the Earth Science Laboratory under contract No. DE-AC07-78ET-28392.

REFERENCES

Cameron, K. L., Cameron, M., Bagby, W. C., Mall, E. J., and Drake, R. E., 1980, Petrologic characteristics of mid-Tertiary volcanic suites, Chihuahua, Mexico: Geology, v. 8, p. 87-91.

Chayes, F., 1969, The chemical composition of Cenozoic andesite, in Proceedings of the Andesite Conference: State of Oregon, Department of Geology and Mineral Resources, Bull. 65, 193 p.

Chevron Resources Co., 1979: Open-file data released by Earth Science Laboratory, Salt Lake City, Utah.

Eakin, T. E., and Lamke, R. D., 1966, Hydrologic reconnaissance of the Humboldt River Basin, Nevada: Nevada Department of Conservation and Natural Resources, Water Resources Bulletin No. 32, 107 p.

Edmiston, R. C., 1979, Ore deposits as exploration models for geothermal reservoirs in carbonate rocks in the eastern Great Basin: Geothermal Resources Council Transactions, v. 3, p. 181-184.

Erwin, J. W., 1974, Bouguer gravity map of Nevada, Winnemucca Sheet; Nevada Bur. Mines Geol., Map 47.

Evans, J. G., and Theodore, T. G., 1978, Deformation of the Roberts Mountains allochthon in north-central Nevada: U.S. Geol. Survey, Prof. Paper 1060.

Fournier, R. O., 1979, Geochemical and hydrologic considerations and the use of enthalpy-chloride diagrams in the prediction of underground conditions in hot-spring conditions: Jour. Volc. and Geoth. Res., v. 5, p. 1-16.

Garbrecht, D. A., 1978, Lineaments in north-central Nevada and their relationship to geothermal areas: University of Nevada-Reno, Masters Thesis, 37 p.

Garside, L. J., 1974, Geothermal exploration and development in Nevada through 1973: Nevada Bur. Mines Geol. Report 21, 12 p.

Garside, L. J., and Schilling, 1979, Thermal waters of Nevada: Nevada Bur. Mines Geol., Bull. 91, 163 p.

Gilluly, J., and Gates, O., with sections by Plouff, D., and Ketner, K. B., 1965, Tectonic and igneous geology of the northern Shoshone Range Nevada: U.S. Geol. Survey, Prof. Paper 465, 153 p.

Gilluly, J., and Masursky, H., 1965, Geology of the Cortez Quadrangle: U.S. Geol. Survey, Bull. 1175, 117 p.

Hose, R. K., and Taylor, B. E., 1974, Geothermal systems of northern Nevada: U. S. Geol. Survey, Open-File Report 74-271, 27 p.

Kuno, H., 1969, Andesite in time and space, in Proceedings of the Andesite Conference: State of Oregon, Department of Geology and Mineral Resources, Bulletin 65, 193 p.

Lawrence Berkeley Laboratory, Geothermal Fluid Data File, Revision 6-14-77.

Mabey, D. R., 1964, Gravity map of Eureka County and adjoining areas, Nevada: U. S. Geol. Survey, Geophysical Investigations Map GP-415.

Mariner, R. H., Presser, T. S., Rapp, J. B., and Willey, L. M., 1974, Chemical properties of some of the major hot springs of northern Nevada: Geol. Soc. Amer. Abstracts with Programs for 1974, Cordilleran Section, Las Vegas, Nevada.

Mariner, R. H., Rapp, J. B., Willey, L. M., and Presser, T. S., 1974, The chemical composition and estimated minimum thermal reservoir temperatures of the principal hot springs of northern and central Nevada: U. S. Geol. Surv., Open-File Report 74-1066, 32 p.

McKee, E. H., and Silberman, M. L., 1970, Geochronology of Tertiary igneous rocks in Central Nevada: Geol. Soc. Amer. Bull., v. 81, p. 2317-2327.

McKee, E. H., Silberman, M. L., Marvin, R. E., and Obradovich, J. D., 1971, A summary of radiometric ages of Tertiary volcanic rocks in Nevada and eastern California. Part I: Central Nevada: Isochron/West, no. 2, p. 21-42.

Muffler, L. J. P., 1964, Geology of the Frenchie Creek Quadrangle, north-central Nevada: U.S. Geol. Surv., Bull. 1179, 99 p.

Muffler, L. J. P., (ed), 1978, Assessment of geothermal resources of the United States: U. S. Geol. Surv., Circular 790, 163 p.

Nockolds, S. R., 1954, Average chemical compositions of some igenous rocks: Geol. Soc. Amer. Bull., v. 65, p. 1007-1032.

Nolan, T. B., and Anderson, G. H., 1934, The geyser area near Beowawe, Eureka County, Nevada: Amer. Jour. Sci., 5th ser., v. 27, 215-229.

Oesterling, W. A., 1960, Areal geology of the Geysers and vicinity, Eureka and Lander Counties, Nevada: geologic map, Southern Pacific Co. Mineral Resource Survey.

Oesterling, W. A., 1962, Geothermal power potential of northern Nevada: Southern Pacific Co. Report.

Olmstead, F. H., Glancy, P. A., Harrill, J. R., Rush, F. E., and Van Denburgh, A. S., 1973, Sources of data for evaluation of selected geothermal areas in northern and central Nevada: U.S. Geol. Survey, Water-Resources Investigations 44-73.

Renner, J. L., White, D. E., and Williams, D. L., 1975, Hydrothermal convection systems, in Assessment of Geothermal Resources of the United States-1975 (eds. D. E. White and D. L. Williams): U. S. Geol. Surv., Circ. 72b, 5-57.

Rinehart, J. S., 1968, Geyser activity near Beowawe, Eureka County, Nevada: Jour. Geoph. Res., v. 73. no. 24, p. 7703-7706.

Roberts, R. J., Montgomery, K. M., and Lehner, R. E., 1967, Geology and Mineral Resources of Eureka County, Nevada: Nevada Bur. Mines Geol., Bull. 64.

Robinson, R. H., 1979, Geothermetric analysis of water samples from Whirlwind Valley, Eureka and Lander Counties, Nevada: Geothermal Resources Council Transactions, v. 3, p. 587-590.

Slemmons, D. B., Jones, A. F., and Gimlett, J. I., 1965, Catalog of Nevada earthquakes: Bull. Seism. Soc. Amer., v. 55, p. 537-583.

Smith, C., 1979, Interpretation of electrical resistivity and shallow seismic reflection profiles, Whirlwind Valley and Horse Heaven areas, Beowawe KGRA, Nevada: Earth Science Lab., Rept. 25, 43 p.

Smith, C., Struhsacker, E. M., and Struhsacker, D. W., 1979, Structural inferences from geologic and geophysical data at Beowawe KGRA, north-central Nevada: Geothermal Resources Council Transactions, v. 3, p. 659-662.

Spurck, W. H., 1960, Geology and mineral resources of Township 32 North, Ranges 45 and 46 East, Mount Diablo base and meridian, Lander County: Nevada, Southern Pacific Co. Report.

Spurck, W. H., 1960, Geology and mineral resources of Township 32 North, Ranges 47 and 48 East, Mount Diablo base and meridian, Lander and Eureka Counties: Southern Pacific Co. report with map.

Stewart, J. H., 1969, Geologic map of the Battle Mountain and part of the Dunphy Quadrangles, Nevada: U. S. Geol. Survey Open-File Rept 69-267.

Stewart, J. H., Walkder, G. W., and Kleinhampl, F. I., 1975, Oregon-Nevada Lineament: Geology, v. 3, (5), p. 265-268.

Stewart, J., and Carlson, J. E., 1976, Cenozoic rocks of Nevada, four maps and brief description of distribution lithology, age, and centers of volcanism: Nev. Bur. Mines Geol., Map 52.

Stewart, J. H., and Carlson, J. E., 1976, Geologic map of north-central Nevada: Nev. Bur. Mines Geol., Map 50.

Stewart, J. H., McKee, E. H., and Stager, H. K., 1977, Geology and mineral deposits of Lander Co., Nevada: Nevada Bur. Mines Geol., Bull. 88.

Swift, C. M., Jr., 1979, Geophysical data, Beowawe geothermal area, Nevada: Geothermal Resources Council Transactions, v. 3, p. 701-704.

Trexler, D. T., Bell, E. J., and Roquemore, G. R., 1977, Evaluation of lineament analysis as an exploration technique for geothermal energy, western and central Nevada: DOE/NVO/0671-2, 77 p.

Wallace, R. E., 1977, Profiles and ages of young fault scarps, north-central Nevada: Geol. Soc. Amer. Bull. v. 88, p. 1267-1281.

Wallace, R. E., 1979, Map of young fault scarps related to earthquakes in north-central Nevada: U. S. Geol. Survey, Open-File Report 79-1554.

Wells, J. D., and Silberman, M. L., 1973, K-Ar age of mineralization at Buckhorn, Eureka Co., Nevada: Isochron/West, no. 8, p. 37-38.

Willson, R. E., 1960, Geology and mineral resources of Township 31 North Range 49 East, Mount Diablo base and meridian, Eureka County, Nevada: Southern Pacific Co. Report.

Wollenburg, H. A., Asaro, F., Bowman, H., McEvilly, T., Morrison, F., and Witherspoon, P., 1975, Geothermal Energy Resource Assessment, Energy and Environment Division: Lawrence Berkeley Laboratory, University of California, UCID-3762, 92 p.

Wollenburg, H., Bowman, H., and Asaro, F., 1977, Geochemical studies at four northern Nevada hot springs areas: Lawrence Berkeley Lab., report LBL-6808, 69 p.

Wrucke, C. T., and Silberman, M. L., 1975, Cauldron subsidence of Oligocene age at Mt. Lewis, Northern Shoshone Range, Nevada: U. S. Geol. Surv., Prof. Paper 876, 20 p.

Zoback, M. L. C., 1978, Mid-Miocene rifting in north-central Nevada: A detailed study of late Cenozoic deformation in the northern basin and range: Ph.D. thesis, Stanford University, 247 p.

Zoback, M. L., 1979, A geologic and geophysical investigation of the Beowawe geothermal area, north-central Nevada: Stanford University Publications, Geological Sciences, v. 16, 79 p.

Zoback, M. L., and Thompson, G. A., 1978, Basin and range rifting in northern Nevada: Clues from a mid-Miocene rift and its subsequent offsets: Geology, v. 6, p. 111-116.

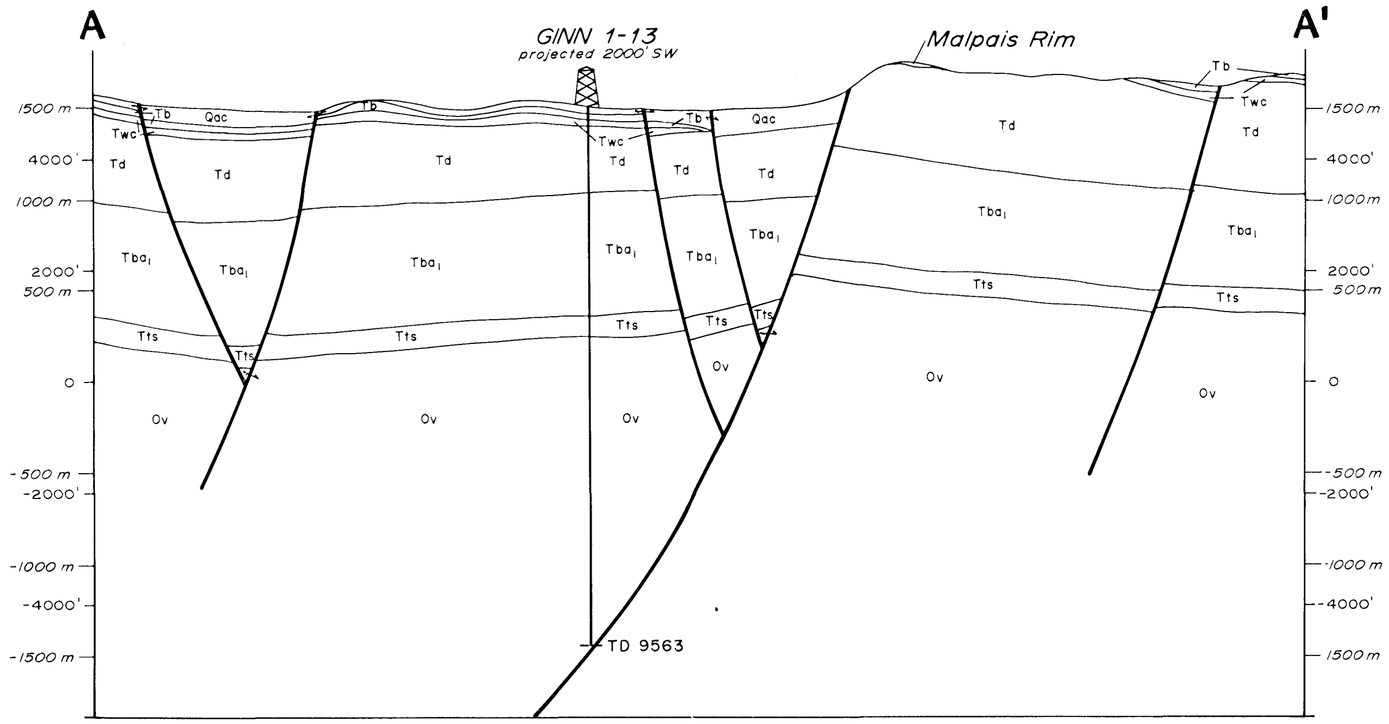

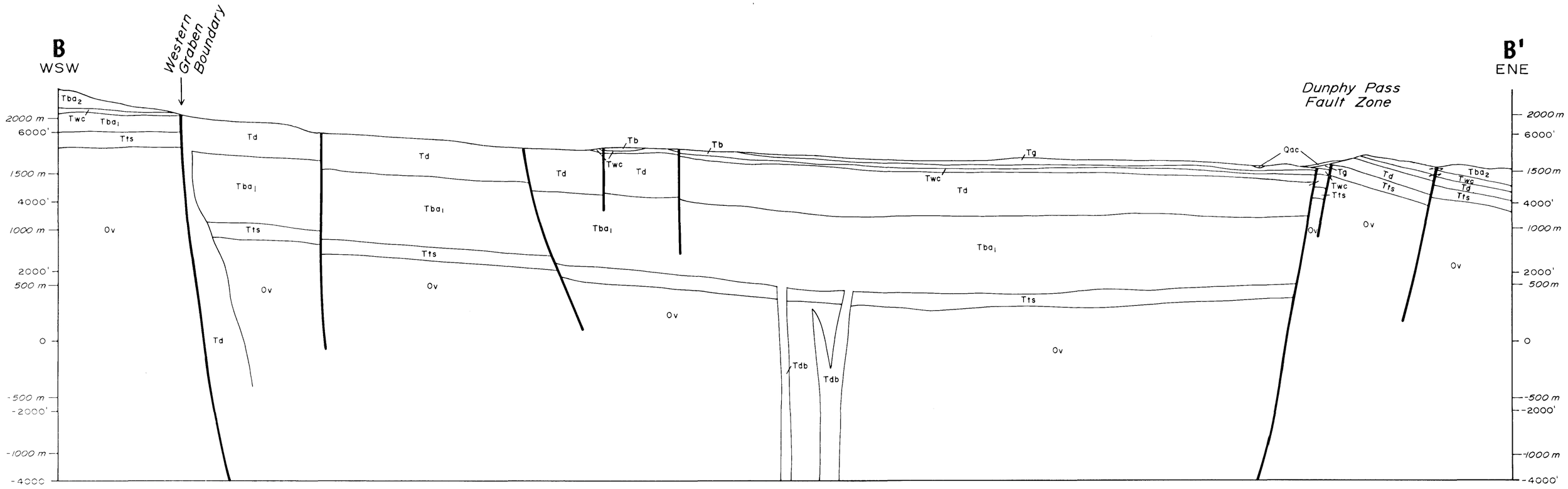

EARTH SCIENCE LABORATORY
UNIVERSITY of UTAH RESEARCH INSTITUTE

SCALE 1:24,000
1/2 0 1 MILE
1000 0 1000 2000 3000 4000 5000 6000 7000 FEET
.5 0 1 KILOMETER
no vertical exaggeration

CROSS SECTIONS OF THE BEOWAWE GEOTHERMAL AREA EUREKA AND LANDER COUNTIES, NEVADA

ERIC M. STRUHSACKER 1980

EXPLANATION

PLIOCENE – QUATERNARY

Qs Upalting Sinter (Quaternary)
Mainly laminated opal with layers of opal-cemented sinter clasts and colluvium.

Qls Landslide Deposits (Quaternary)

Qac Alluvium and Colluvium (Quaternary)

Tg Coarse Gravel (Miocene - Pliocene)
Contains cobbles and pebbles of pyroxene dacite (Td), young basaltic andesite (Tba), and late basalt (Tb).

Tb Late Basalt (Miocene)
Thin flows of black dictyotaxitic basalt containing occasional macroscopic grains of olivine set in a subophitic matrix of plagioclase and clinopyroxene. The flows display crude columnar to blocky jointing. The K-Ar age is 15.5 ± 0.8 m.y.

Tba2 Young Basaltic Andesite (Miocene)
Thin flows of brown to black basaltic andesite with plagioclase and olivine phenocrysts set in a felty matrix of plagioclase, clinopyroxene, and brown glass. The flows display crude blocky jointing. The K-Ar age is 15.7 ± 0.7 m.y.

MIDDLE MIOCENE

Twc White Canyon Tuffaceous Sedimentary Rocks (Miocene)
Well bedded buff to grey tuffaceous gravel, sandstone, siltstone, poorly consolidated pyroclastic deposits, and porcellanite. Gravel and sandstone conprise most of the unit and contain clasts of pyroxene dacite (Td) and basaltic andesite, broken quartz and feldspar phenocrysts, and abundant subaligned brown to black glass shards with a few intact bubble walls. Pumice clasts abundant near the top of the unit.

Td Pyroxene Dacite (Miocene)
Lower portion of the unit contains thick flows of plagioporphyritic dacite with abundant aggregates of plagioclase, pyroxene, olivine and magnetite phenocrysts in a glassy groundmass. Some flows contain sanidine microlites as well. Flows of black spherulodial vitrophyre cap the dacite porphyry. The upper portion of the unit contains thin flows of intermediate black and red-brown aphanitic dacite with sparse phenocrysts of plagioclase and abundant magnetite. The red-brown flows display platey jointing. The K-Ar age is 16.1 ± 0.8 m.y.

LOWER MIOCENE

Tba1 Old Basaltic Andesite (Miocene?)
A grey to black sequence of mafic lava flows which range in composition from basalt to andesite. The flows contain plagioclase phenocrysts set in a matrix of plagioclase, pyroxene, and minor olivine. Sequence contains interflow rubble zones and felsic tuffs.

Tts Old Tuffaceous Sedimentary Rocks (Oligocene-Miocene)
The unit contains interbedded tuffaceous layers of gravel, sand, and silt. The matrix of these beds contains broken feldspar, quartz, and mafic crystals with well-preserved glass shards. The gravel layers contain abundant siliceous pebbles from the Valy Formation with lesser amounts of felsic and mafic volcanic clasts. Buff to grey ash layers occur intermittently.

Tha An interbedded hornblende biotite andesite flow (38.6 ± 1.3 m.y.) occurs in the lower portion of the unit. The rock contains 20% plagioclase, 15% hornblende, and 3% biotite as amedrol phenocrysts in a light gray microlitic to aphanitic groundmass. Magnetite is common as disseminated grains. Volcanic xenoliths are common.

ORDOVICIAN

Ov Valley Formation (Ordovician)
Predominantly light grey siliceous siltstone with inlck horizons of quartzite, sandstone, bedded chert, and siliceous conglomerate.

MAP SYMBOLS

Contact, dashed where approximately located.

Normal fault, dashed (long) where approximately located, dotted where concealed, ball indicating dip of fault plane, dashed (short) where inferred from geophysics.

Strike and dip of beds and flow horizons.

Deep geothermal well.

●154 K-Ar age date sample location.

EARTH SCIENCE LABORATORY
UNIVERSITY of UTAH RESEARCH INSTITUTE

SCALE 1:24,000
1/2 0 MILE
1000 0 1000 2000 3000 4000 5000 6000 7000 FEET
1 .5 0 KILOMETER

GEOLOGIC MAP OF THE BEOWAWE GEOTHERMAL AREA EUREKA AND LANDER COUNTIES, NEVADA

ERIC M. STRUHSACKER 1980

APPROXIMATE MEAN DECLINATION, 1970

PHOTOGEOLOGY WITH FIELD CHECKS
DETAILED MAPPING